

**DEVOLATILIZATION STUDIES OF OIL PALM
PLANTATION RESIDUES VIA TORREFACTION
PROCESS**

TEO YU XUN

**BACHELOR OF CHEMICAL ENGINEERING
UNIVERSITI MALAYSIA PAHANG**

©TEO YU XUN (2015)

Thesis Access Form

No _____ Location _____

Author :

Title :

Status of access OPEN / RESTRICTED / CONFIDENTIAL

Moratorium period: _____ years, ending _____ / _____ 200_____

Conditions of access proved by (CAPITALS): DR. SAIDATUL SHIMA BINTI JAMARI

Supervisor (Signature).....

Faculty:

Author's Declaration: *I agree the following conditions:*

OPEN access work shall be made available in the Universiti Malaysia Pahang only and not allowed to reproduce for any purposes.

The statement itself shall apply to ALL copies:

This copy has been supplied on the understanding that it is copyright material and that no quotation from the thesis may be published without proper acknowledgement.

Restricted/confidential work: All access and any photocopying shall be strictly subject to written permission from the University Head of Department and any external sponsor, if any.

Author's signature.....Date:

users declaration: for signature during any Moratorium period (Not Open work):

I undertake to uphold the above conditions:

Date	Name (CAPITALS)	Signature	Address

DEVOLATILIZATION STUDIES OF OIL PALM PLANTATION RESIDUES VIA TORREFACTION PROCESS

TEO YU XUN

Thesis submitted in partial fulfilment of the requirements
for the award of the degree of
Bachelor of Chemical Engineering

**Faculty of Chemical & Natural Resources Engineering
UNIVERSITI MALAYSIA PAHANG**

JANUARY 2015

©TEO YU XUN (2015)

SUPERVISOR'S DECLARATION

We hereby declare that we have checked this thesis and in our opinion, this thesis is adequate in terms of scope and quality for the award of the degree of Bachelor of Chemical Engineering.

Signature :
Name of main supervisor : DR. SAIDATUL SHIMA BINTI JAMARI
Position : SENIOR LECTURER
Date :

STUDENT'S DECLARATION

I hereby declare that the work in this thesis is my own except for quotations and summaries which have been duly acknowledged. The thesis has not been accepted for any degree and is not concurrently submitted for award of other degree.

Signature :
Name : TEO YU XUN
ID Number : KA11119
Date :

Dedication

*Highest gratitude to
my supervisor, my family members and my friends
for all your care, support and trust on me.*

*Special dedication to
Faculty of Chemical Engineering and Natural Resources of
University Malaysia Pahang
on providing all the related environment
and appropriate equipment
on finishing my research.*

ACKNOWLEDGEMENT

First and foremost, I would like to dedicate the most sincere gratitude to my supervisor, Dr. Saidatul Shima binti Jamari for her guidance through an effective well-arranged weekly meeting. She had always offered me a helping hand and never failed to share her knowledge.

Next, I would like to thank the Faculty of Chemical and Natural Resources of University Malaysia Pahang in providing me a superb environment of study and learning throughout the research.

Last but not least, I would also like to express my gratitude towards my friends and family members for their support and encouragement which helps me in completing this project.

ABSTRACT

Biomass represents a type of renewable energy source that will play a substantial role in the future global energy balance in terms of energy security and carbon-neutral fuel. However, raw lignocellulosic biomass presents several undesired properties such as low energy density, hygroscopic nature, and low bulk density that do not permit its direct exploitation. Torrefaction, an emerging thermal pretreatment process, is acknowledged to improve the fuel properties of raw biomass towards an efficient renewable energy supply. This paper investigates the fuel characteristics of OPF and OPT at temperatures: 200°C, 250°C, and 300°C at a constant heating rate of 10°C/min and 30 min residence time. The torrefied products were characterized in terms of their moisture content, calorific value, mass and energy yield. Prediction of calorific value based on the colour of torrefied biomass was also presented here. Bomb calorimeter was used to measure the calorific value in order to calculate mass and energy yield for analysis. In addition, Fourier Transform Infrared (FTIR) Spectroscopy, Thermogravimetric Analysis (TGA), and Derivative Thermogravimetric (DTG) analysis were performed to investigate the changes of lignocellulosic physicochemical properties of the studied materials. As a result, both OPF and OPT with calorific value of 16.41 MJ/kg and 17.41 MJ/kg were improved to 22.46 MJ/kg and 25.48 MJ/kg respectively after torrefaction at 300°C. The mass yield for both samples decrease at elevated torrefaction temperature while retaining their energy yield between 90-100%. The degradation behaviours of lignocellulosic components: hemicellulose, cellulose, and lignin were discussed through FTIR, TGA, and DTG analysis. Meanwhile, the improved hydrophobic characteristic was also justified. This work concludes that OPF and OPT made a good biomass for torrefaction purpose which can be upgraded to universal energy commodity.

ABSTRAK

Biojisim mewakili sejenis sumber tenaga yang boleh diperbaharui dan ia memainkan peranan penting dalam imbangan tenaga global masa hadapan dari segi keselamatan tenaga dan sebagai bahan api karbon-neutral. Walau bagaimanapun, biojisim lignoselulosik mentah mempunyai beberapa karakteristik yang tidak diingini seperti kepadatan tenaga yang rendah, sifat hidroskopis, dan ketumpatan pukal yang rendah serta tidak membenarkan eksploitasi langsung. Torrefaksi adalah satu proses prarawatan termal untuk meningkatkan sifat-sifat bahan api biojisim mentah ke arah bekalan tenaga yang boleh diperbaharui dan cekap. Kertas ini mengkaji ciri-ciri bahan api OPF dan OPT pada suhu torrefaction: 200°C, 250°C, 300°C pada kadar pemanasan 10°C/min dengan masa tinggal 30 min. Produk torrefaksi telah dicirikan dari segi kandungan kelembapan, nilai kalori, jisim dan hasil tenaga. Ramalan nilai kalori berdasarkan warna biojisim torrefaksi telah juga dibentangkan. Bom kalorimeter digunakan untuk mengukur nilai kalori bagi mengira jisim dan tenaga hasil untuk analisis. Di samping itu, Fourier Transform Infrared (FTIR) Spektroskopi, Analisis Termogravimetri (TGA), dan derivatif Termogravimetri (DTG) analisis telah dijalankan untuk menyiasat perubahan sifat fizikokimia lignoselulosa daripada bahan yang dikaji. Akibatnya, kedua-dua OPF dan OPT dengan nilai kalori 16.41 MJ/kg dan 17.41 MJ/kg telah meningkat kepada 22.46 MJ/kg dan 25.48 MJ/kg masing-masing selepas torrefaksi pada suhu 300°C. Hasil massa untuk kedua-dua sampel dikurangkan apabila suhu torrefaksi meningkat, pada masa yang sama hasil tenaga mereka dikekalkan di antara 90-100%. Tingkah laku degradasi komponen lignoselulosa: hemiselulosa, selulosa, lignin dan telah dibincangkan melalui analisis FTIR, TGA, dan DTG. Sementara itu, ciri hidrofobik yang bertambah baik juga telah diwajarkan. Kerja ini menyimpulkan bahawa OPF dan OPT merupakan biojisim baik untuk tujuan torrefaction yang boleh dinaik taraf kepada komoditi tenaga universal.

TABLE OF CONTENTS

SUPERVISOR'S DECLARATION	IV
STUDENT'S DECLARATION	V
Dedication	VI
ACKNOWLEDGEMENT	VII
ABSTRACT	VIII
ABSTRAK	IX
TABLE OF CONTENTS	X
LIST OF FIGURES	XII
LIST OF TABLES	XIV
LIST OF SYMBOLS	XV
LIST OF ABBREVIATIONS	XVI
1 INTRODUCTION	1
1.1 Motivation and statement of problem	1
1.2 Objectives	3
1.3 Scope of this research	3
1.4 Organisation of this thesis	3
2 LITERATURE REVIEW	5
2.1 Overview	5
2.2 Biomass	5
2.3 Properties of Lignocellulosic Biomass	7
2.3.1 Cellulose	9
2.3.2 Hemicellulose	9
2.3.3 Lignin	10
2.4 Palm oil and Oil Palm Biomass in Malaysia	11
2.4.1 Oil Palm Fronds (OPF)	13
2.4.2 Oil Palm Trunks (OPT)	14
2.5 Biomass Conversion Methods	15
2.5.1 Biochemical Conversions	16
2.5.2 Thermochemical Conversions	16
2.6 Torrefaction	19
2.6.1 Mechanism of Torrefaction	20
2.6.2 Effect of Operating Parameters	21
2.6.3 Effect of Biomass Colour on Calorific Value	25
2.7 Summary	26
3 MATERIALS AND METHODS	27
3.1 Overview	27
3.2 Raw Materials	27
3.3 Chemical	29
3.4 Torrefaction Process	29
3.5 Calorific value Prediction using RGB Colour Model	30
3.6 Characterizations	33
3.6.1 Moisture Content	33
3.6.2 Calorific Value	34
3.6.3 Fourier Transform Infrared (FTIR) Spectroscopy	37

3.6.4	Thermogravimetric Analysis (TGA)	37
3.7	Mass and Energy Yield	38
4	RESULTS AND DISCUSSION	39
4.1	Overview	39
4.2	Preliminary Results on Moisture Content and Calorific Value	39
4.3	Predicted Calorific Value of Torrefied Biomass based on Colour	40
4.4	Effect of Temperature on the Calorific Value.....	42
4.5	Effect of Temperature on the Mass and Energy Yields	43
4.6	Fourier Transform Infrared (FTIR) Analysis	45
4.7	Thermogravimetric Analysis (TGA).....	47
5	CONCLUSION AND RECOMMENDATION.....	51
5.1	Conclusion.....	51
5.2	Recommendation.....	52
	APPENDICES	60
	Appendix A.1: Summary of experimental results.....	60
	Appendix A.2: Characteristic of IR Absorptions / Transmittances	65
	Appendix A.3: Colour Characterization Data.....	66

LIST OF FIGURES

Figure 2-1: Steps of photosynthetic biomass growth (Demirbas, 2009)	6
Figure 2-2: Lignocellulosic structure of plant biomass (Tomme <i>et al.</i> , 1995)	8
Figure 2-3: Chemical structure of cellulose (Nhuchhen <i>et al.</i> , 2014).....	9
Figure 2-4: Chemical Structure of Hemicellulose: (a) Softwood; (b) Hardwood (Dhepe & Sahu, 2012)	10
Figure 2-5: Three basic monomers of lignin (Albizati & Tracewell, 2012).....	11
Figure 2-6: Crude palm oil (CPO) production and plantation area in Malaysia (Aljuboori, n.d.)	13
Figure 2-7: Oil palm biomass residue and source of generation	13
Figure 2-8: Biomass conversion methods in two major paths (Basu, 2010)	15
Figure 2-9: Pyrolysis of a biomass particle (Basu, 2010).....	18
Figure 2-10: Weight loss in terms of cellulose, hemicellulose, and lignin (Basu, 2010).....	21
Figure 2-11: Weight loss of condensed liquid with residence time (Chen <i>et al.</i> , 2011).	23
Figure 2-12: Colour change during torrefaction process (Stelte <i>et al.</i> , 2011)	25
Figure 2-13: Colour of lignocellulosic material (a) Soft: rice straw (b) Hard: palm kernel shell (PKS).....	26
Figure 3-1: OPF fibres produced from press machine.....	28
Figure 3-2: OPF and OPT fibres in desired size	28
Figure 3-3: Stainless steel reactor and its support ring.....	29
Figure 3-4: Schematic diagram of experimental setup	30
Figure 3-5: RGB colour model	31
Figure 3-6: Colour picking software – Pixeur v3.2 (Veign, 2009).....	32
Figure 3-7: CV Predictor created using Microsoft Excel spreadsheet.....	32
Figure 3-8: Electronic Balance in FKKS Environmental Engineering Lab	33
Figure 3-9: Electric Oven in FKKS Environmental Engineering Lab.....	34
Figure 3-10: Structure of Bomb Calorimeter.....	36
Figure 4-1: Raw and torrefied OPF samples	41
Figure 4-2: Raw and torrefied OPT samples	41
Figure 4-3: Effect of temperature on predicted and average experimental calorific value	42
Figure 4-4: Effect of temperature on OPF mass and energy yields (average).....	43
Figure 4-5: Effect of temperature on OPT mass and energy yields (average)	44
Figure 4-6: FTIR spectra for raw and torrefied OPF at different operating temperature.....	46
Figure 4-7: FTIR spectra for raw and torrefied OPT at different operating temperature.....	47
Figure 4-8: TGA curves of raw and torrefied OPF at different operating temperature ..	48

Figure 4-9: DTG curves of raw and torrefied OPF at different operating temperature.. 48

Figure 4-10: TGA curves of raw and torrefied OPT at different operating temperature 49

Figure 4-11: DTG curves of raw and torrefied OPT at different operating temperature 49

LIST OF TABLES

Table 2-1: General classification of biomass resources (EUBIA, 2012).....	7
Table 2-2: Polymeric constituents of various materials (Sun & Cheng, 2002)	8
Table 2-3: Chemical compositions of OPF.....	14
Table 2-4: Chemical compositions of OPT	15
Table 2-5: Comparison in four main thermochemical treatment processes (Demirbas, 2009)	17
Table 2-6: Temperature range for thermal degradation of cellulose, hemicellulose and lignin	22
Table 2-7: Mass loss in polymeric components at different temperatures (Chen & Kuo, 2011)	23
Table 4-1: Moisture content (MC) for raw materials	39
Table 4-2: Calorific value for raw materials.....	40
Table 4-3: Results of RGB index and predicted CV	41
Table 4-4: Comparison between experimental and predicted CV	42
Table 4-5: Vibration intensity of functional groups for raw and torrefied products	46

LIST OF SYMBOLS

<i>CV</i>	<i>Calorific value</i>
<i>e₁</i>	correction in calories for heat of formation of nitric acid
<i>e₂</i>	correction in calories for heat of formation of sulfuric acid
<i>e₃</i>	correction in calories for heat of combustion of fuse wire
<i>m</i>	mass of sample
<i>t</i>	temperature rise
<i>W</i>	constant of eq.(3.2)

LIST OF ABBREVIATIONS

CPO	Crude palm oil
CV	Calorific value
DTG	Derivative Thermogravimetric
EFB	Empty fruit bunch
FFB	Fresh fruit bunch
FTIR	Fourier Transform Infrared
GHG	Greenhouse gas
HHV	Higher heating value
MC	Moisture content
OPF	Oil palm frond
OPT	Oil palm trunk
PKS	Palm kernel shell
POME	Palm oil mil effluent
TG	Thermogravimetric
TGA	Thermogravimetric Analysis

1 INTRODUCTION

1.1 Motivation and statement of problem

World primary energy demand, reported as 524 quadrillion British thermal units (Btu) in 2010, is expected to increase by 56% in 2040 (EIA, 2013). Energy security and environmental sustainability are major emerging issues which can only be addressed through diversification in energy resources and clean fuels. The extent of greenhouse gas (GHG) emission by fossil fuel is so significant due to the urgent need to reduce the carbon footprint of the world via the usage of alternative energy sources that are benign to the environment (Ossai *et al.*, 2013). The growing concerns about future depletion of fossil fuels and accumulation of their emissions in the environment have attracted world's attention to exploit and utilize renewable energy sources and low carbon fuels. It is realized that a continuous reliance on fossil fuels will have catastrophic results because excessive carbon dioxide emission has dramatic global warming effects (Awan & Khan, 2014). Volatility of oil prices and its high demand have also encouraged global community to reduce the dependence on oil and replace it with clean and renewable energy resources (Fauzianto, 2014). On the other hand, the implementation of national targets to increase the amount of renewable energy and reduce GHG emissions is accelerating the utilization of resources such as solar, wave, wind, tidal, and biomass. These resources have their own unique advantages and disadvantages.

Biomass is a unique renewable resource. It appears to be a promising alternative energy resource to replace fossil fuels in the future. As a sustainable carbon carrier, biomass, unlike fossil fuels, is planted and collected annually which provides a continuous energy supply. Biomass is a carbon-neutral fuel as its carbon is recycled from the atmosphere. In addition, biomass can exist in the form of solid (briquette, pellet, char), liquid (biodiesel, ethanol), or gaseous (biogas) fuel which makes it ideal for 100% renewable energy systems as it can be fully utilized in heat and electricity generation, and even the transport sectors (Mathiesen *et al.*, 2012). Therefore, biomass plays a substantial role in the future energy scenarios.

Biomass however, presents several undesired properties that do not permit its direct exploitation. Raw biomass is classified as low grade fuel that associates with several

shortcomings like structural heterogeneity, non-uniform physical properties, low energy density, hygroscopic nature, and low bulk density. These drawbacks create difficulties in several aspects such as transportation, storage complications, lower thermal-conversion efficacy and utilization limitations (Xue *et al.*, 2014). In order to overcome these problems, the properties of raw biomass need to be modified. A viable option is to carry out a thermochemical pre-treatment process, specifically the torrefaction process.

Torrefaction is a mild pyrolysis process which undergoes thermal decomposition of biomass in the inert atmosphere with the absence of oxygen. It is characterized by low particle heating rate (<50°C/min) with an operating temperature typically ranging from 200°C to 300°C and a residence time not more than one hour (Chen & Kuo, 2010). The biomass partly decomposes, giving off various types of volatiles during the process. The solid product, namely torrefied biomass will result in loss of mass and chemical energy to the gas phase, leaving a biomass with improved properties which make it attractive for further utilizations such as combustion and gasification in general (Baskar *et al.*, 2012).

Oil palm (*Elaeis guineensis*) is an agro-industrial commodity and the principal source of palm oil. Malaysia, as the second largest oil palm-producing country that comes after Indonesia, accounts for 39% of world's palm oil production and 44% of world's exports (MPOC, 2009). There are abundant raw materials available from the oil palm trees which constitute a 10% of oil and the rests are classified as biomass residues (Abdullah & Sulaiman, 2013). These residues can be sorted into two types: oil palm plantation residues consisting of oil palm fronds (OPF) and oil palm trunks (OPT), as well as oil palm mill residues consisting of empty fruit bunches (EFB), palm kernel shells (PKS), mesocarp fibre, and palm oil mill effluent (POME). In order to seek benefits from these biomass residues, several researches have examined the potential of energy generation from these agricultural wastes (Lai & Idris, 2013; Lu *et al.*, 2012; Peng *et al.*, 2012; Sulaiman *et al.*, 2009; Van der Stelt *et al.*, 2011; Wannapeera *et al.*, 2011).

Torrefaction process on oil palm biomass has gained interest among the researchers towards its potential products for energy generation. However, major studies only emphasized on the wastes or by-products obtained from palm oil mills, i.e., EFB, PKS, mesocarp fiber, and POME whereas the wastes obtained from plantation sites such as OPF and OPT are currently underutilized due to the limited knowledge available on

their respective. Hence, this research was experimentally conducted to understand the physical and chemical processes in torrefaction of OPF and OPT as well as to fully utilize its usability and economic value towards a better development of Malaysia in terms of renewable energy source.

1.2 Objectives

The following is the objective of this research:

- To study the torrefaction effect on physicochemical properties of oil palm fronds (OPF) and oil palm trunks (OPT) at different temperature levels

1.3 Scope of this research

The following are the scopes of this research:

- i) Experimental analysis of torrefaction behaviour of OPF and OPT at different temperature ranging within 200–300°C
- ii) Prediction of calorific value at various torrefaction temperature for OPF and OPT based on their colours using RGB colour model
- iii) Characterization of moisture content and calorific value for mass and energy yield analysis
- iv) Characterization analysis on lignocellulosic structure of OPF and OPT via Fourier Transform Infrared (FTIR) Spectrometry and Thermogravimetric Analysis (TGA) for devolatilization studies

1.4 Organisation of this thesis

The structure of the reminder of the thesis is outlined as follow:

Chapter 2 mainly discusses on the information gathered and the reviews related to the topic concerned. It starts with the biomass review in which general information of biomass and its sources are provided. Then, the properties of lignocellulosic biomass and its major constituents (cellulose, hemicellulose, and lignin) are briefly discussed. This is followed by a discussion on the palm oil and oil palm biomass in Malaysia together with oil palm fronds (OPF) and oil palm trunks (OPT) as its subchapters. Several biomass conversion methods and torrefaction process, which is the main study in this research, are also elaborated in detail. Extensive reviews on the operating

parameters affecting the thermal treatment process are also presented. Last but not least, the effect of biomass colour on calorific value is discussed.

Chapter 3 provides a discussion on samples preparation, methods, and measurements applied in this research. The preparation of samples from converting raw materials into desired fibrous samples until storage handling prior to experimental purpose is discussed. This is then followed by a brief discussion on the torrefaction method used in this study. Besides, a detailed discussion on calorific value prediction based on colour of biomass is presented. In addition, this chapter also provides the methods used to characterize moisture content and calorific value, as well as performing FTIR spectrometry and Thermogravimetric Analysis (TGA). Lastly, measurements for mass and energy yield are formulated as well in this chapter.

Chapter 4 is devoted to the results which cover the moisture content, predicted and experimental calorific value, mass and energy yield, FTIR analysis, TG-DTG analysis for both raw and torrefied OPF and OPT. The results are further discussed based on previous studies and researches.

Chapter 5 concluded the results for this work and necessary recommendations are added in order to enhance the future researches related to this work.

2 LITERATURE REVIEW

2.1 Overview

This paper presents the reviews related to the experimental studies of torrefaction process, a thermal pretreatment method to convert raw biomass into added value solid product with enhanced fuel properties. The chapter starts with an informative description of biomass, followed by its lignocellulosic properties that explain the reason of choosing OPF and OPT as raw materials for torrefaction studies in this research. In addition, extensive reviews are made to compare various biomass conversion methods and studies on previous research operating parameters give a better understanding on the effect of temperature towards torrefaction behaviour which in turn led to the objective in this study.

2.2 Biomass

The term biomass (Greek *bio* meaning *life* + *maza* meaning *mass*) refers to any biological matter derived from the living organism such as plants and animals. It is different from the organic materials which have been transformed by geological processes for millions of years into primitive substances such as coal or petroleum (Demirbas, 2009). Biomass is recognized as a renewable energy since solar energy can be stored and converted into chemical energy via photosynthesis during the growth of plants and trees, and then released through direct or indirect combustion for heat and electricity generation. Presence of sunlight triggers the photosynthesis of green plants where water molecules are broken down to obtain electrons and protons that contribute in converting carbon dioxide into glucose and oxygen as the final products (Basu, 2010). During the process, the chlorophyll promotes the absorption of carbon dioxide from the atmosphere which facilitates the growth of the plant. Figure 2-1 displays a summary on the growth of photosynthetic biomass.

Each year, a vast amount of biomass grows through photosynthesis by capturing and concentrating the carbon dioxide directly from the atmosphere. Burning of biomass subsequently releases the carbon dioxide back again to the atmosphere. Thus, any burning of biomass does not add to the Earth's carbon dioxide inventory. For this reason, biomass is said to be "carbon-neutral" (Basu, 2010). Furthermore, due to negligible

amount of sulphur and nitrogen contents, biomass upon burning does not contribute to acid rain gases, thus it is recognized as a clean fuel (Demirbas, 2008).

Biomass encompasses a wide array of materials such as forestry, agricultural, and agro-industrial residues, as well as municipal and industrial wastes. Table 2-1 presents a general classification of biomass types according to their supply sector. Forestry and agriculture sector are two main resources representing the primary sources of biomass whereas industry and waste residues are secondary sources of biomass derived from primary sources.

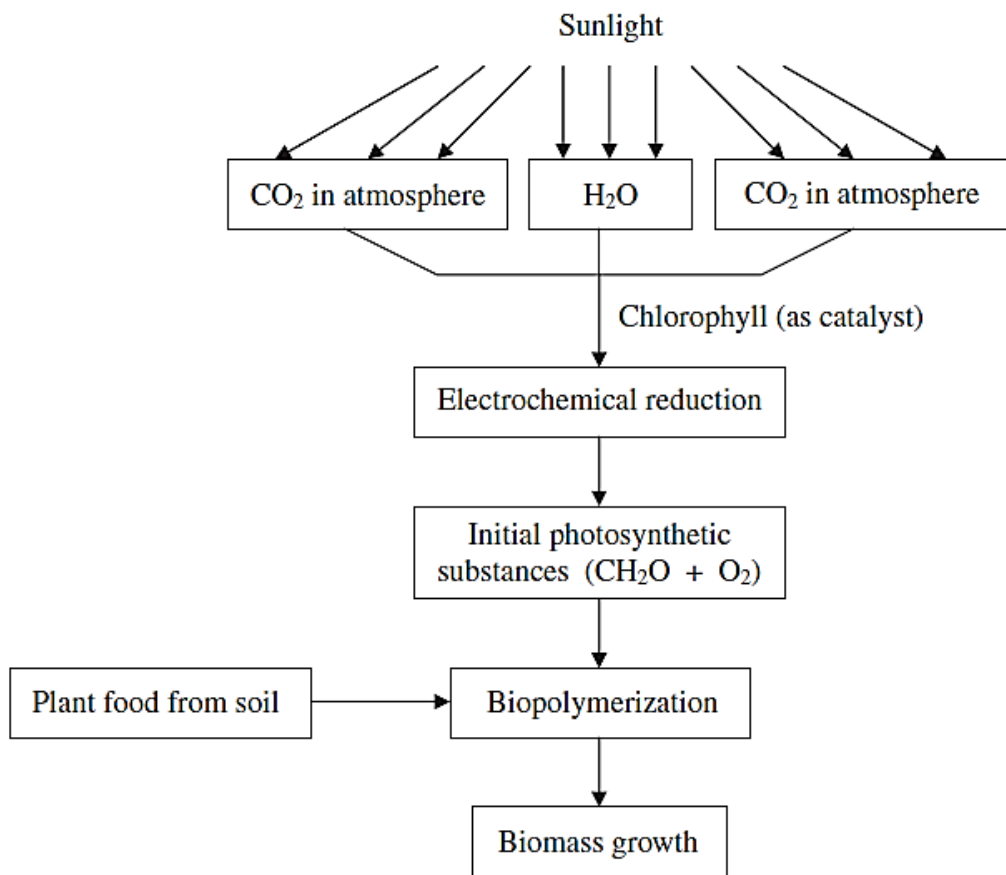


Figure 2-1: Steps of photosynthetic biomass growth (Demirbas, 2009)

Table 2-1: General classification of biomass resources (EUBIA, 2012)

Supply sector	Type	Example
Forestry	Dedicated forestry	Short rotation plantations (e.g. willow, <i>populus</i> , <i>eucalyptus</i>)
	Forestry by-products	Wood blocks, wood chips from thinning
Agriculture	Dry lignocellulosic energy crops	Herbaceous crops (e.g. <i>miscanthus</i> , reed canarygrass, giant reed)
	Oil, sugar and starch from energy crops	Oil seeds for methylesters (e.g. rape seed, sunflower), sugar crops for ethanol (e.g. sugar cane, sweet sorghum), starch crops for ethanol (e.g. maize, wheat)
	Agricultural residues	Straw, prunings from vineyards and fruit trees
	Livestock waste	Wet and dry manure
Industry	Industrial residues	Industrial waste wood, sawdust from sawmills, fibrous vegetable waste from paper industries
Waste	Dry lignocellulosic waste	Residues from parks and gardens (e.g. prunings, grass)
	Contaminated waste	Demolition wood, organic fraction of municipal solid waste, biodegradable landfilled waste, landfill gas, sewage sludge

2.3 Properties of Lignocellulosic Biomass

Biomass can be classified into lignocellulosic or non-lignocellulosic materials. Lignocellulosic materials refer to non-starch and fibrous part of the plants (cell wall) consisting of three major constituents (cellulose, hemicellulose, and lignin) which are strongly intermeshed and chemically bonded (Limayem & Ricke, 2012). On the other hand, non-lignocellulosic materials refer to non-cellulosic organic materials such as sugar (sucrose), starch, protein, and fat (oil) mainly used for nutritional purpose.

In order to achieve an efficient conversion of lignocellulosic biomass, it is necessary to have a better understanding on the cell wall structure and its compositions. The components which constitute the primarily part of a plant's cell wall are three major biopolymers consisting of cellulose, hemicellulose, and lignin as shown in Figure 2-2. Depending on the plant species, there is considerable variation in the relative amounts of each of these biopolymers within the cell walls. The composition, structure, and interactions of these biopolymers composing the lignocellulosic matrix serve many interrelated functions for the plant, including the primary function of providing structural features that create mechanical support, allowing for internal transport of water, nutrients, and photosynthetic products throughout the plant (Wyman, 2013). A

comparison on the amount of each of these polymeric constituents for some principal type of lignocellulosic materials is presented in Table 2-2. In contrast, biomass from animal wastes such as swine waste and solid cattle manure is rather poor in these polymeric constituents which make it a type of an inadequate material for torrefaction process. These polymeric constituents of biomass are further discussed in the subchapter 2.3.1-2.3.3.

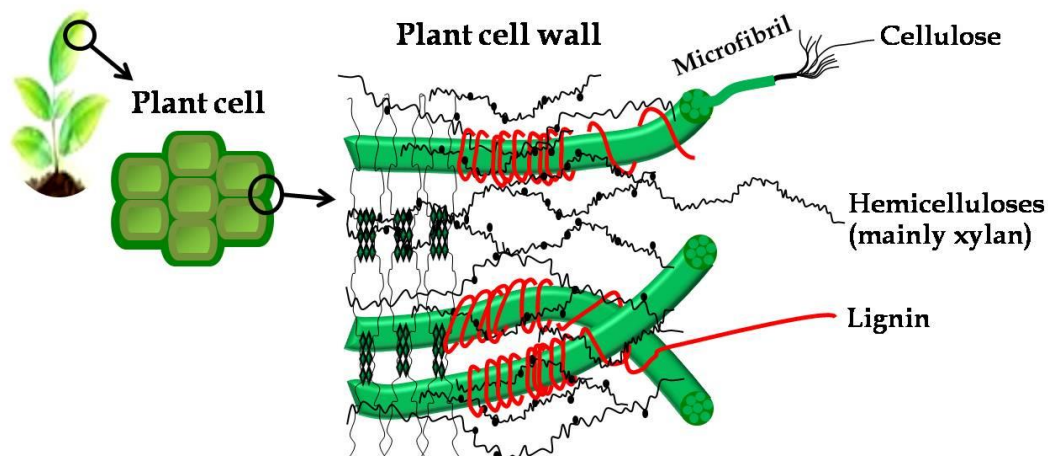


Figure 2-2: Lignocellulosic structure of plant biomass (Tomme *et al.*, 1995)

Table 2-2: Polymeric constituents of various materials (Sun & Cheng, 2002)

Lignocellulosic materials	Cellulose (%)	Hemicellulose (%)	Lignin (%)
Hardwoods stems	40–55	24–40	18–25
Softwood stems	45–50	25–35	25–35
Nut shells	25–30	25–30	30–40
Corn cobs	45	35	15
Grasses	25–40	35–50	10–30
Paper	85–99	0	0–15
Wheat straw	30	50	15
Sorted refuse	60	20	20
Leaves	15–20	80–85	0
Cotton seed hairs	80–95	5–20	0
Newspaper	40–55	25–40	18–30
Waste papers from chemical pulps	60–70	10–20	5–10
Primary wastewater solids	8–15	NA	24–29
Swine waste	6.0	28	NA
Solid cattle manure	1.6–4.7	1.4–3.3	2.7–5.7
Coastal Bermuda grass	25	35.7	6.4
Switch grass	45	31.4	12.0

2.3.1 Cellulose

Cellulose is the main constituent of lignocellulosic biomass due to its large molecular weights of 500,000 units of monomers (Basu, 2010). It is a linear polysaccharide polymer consisting of a linear chain of D-glucose linked by β -(1,4)-glycosidic bonds to each other (Rowell, 2005). Cellulose chains are linked together by a number of intra- and inter-molecular hydrogen bonds as well as van der Waals forces, resulting in the form of microfibrils with high tensile strength (Ha *et al.*, 1998). Figure 2-3 shows the chemical structure of cellulose with different hydroxyl groups in the chain. These hydroxyl groups increase the ability to form hydrogen bonds which enhance the hygroscopic property of lignocellulosic biomass. This hygroscopic (hydrophilic) nature increases the gap between cellulose chains and causes the lignocellulosic biomass to swell when immersed in water. For this reason, biomass may encounter shrinkage phenomena upon thermal treatment, causing dimensional variations and loss of moisture content (Nhuchhen *et al.*, 2014).

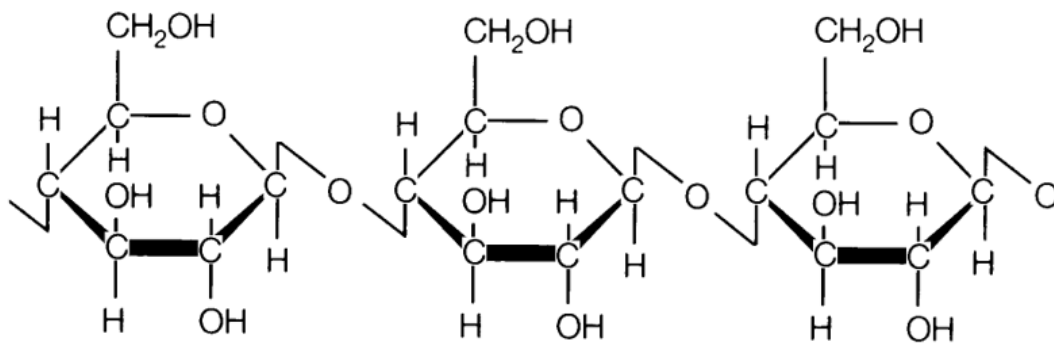


Figure 2-3: Chemical structure of cellulose (Nhuchhen *et al.*, 2014)

2.3.2 Hemicellulose

Hemicellulose is the second most abundant polymers in lignocellulosic biomass. In contrast to cellulose, hemicelluloses are more amorphous, random, and branched heterogenic polysaccharides consisting of various pentoses (xylose and arabinose), hexoses (glucose, galactose, mannose, and/or rhamnose), and acids (glucuronic acid, methyl glucuronic acid, and galacturonic acid) (Girio *et al.*, 2010). Its random and amorphous structure makes it as the weakest constituent of biomass cells (Basu, 2010). Hemicellulose is composed predominantly of methyl- and acetyl- substituted groups which take part in releasing light volatiles gases such as CO and CO₂ upon low temperature thermal pretreatment (Rowell, 2005). Unlike cellulose, hemicellulose has a

lower degree of polymerization that results in substantial thermal degradation. Therefore, it contributes a significant effect on mass yield during torrefaction process. Figure 2-4 (a) and (b) show the hemicellulose structure for softwood and hardwood respectively. The softwood hemicellulose mainly consists of xylose, arabinose, mannose, galactose, and glucuronic acid while hardwood hemicellulose is mainly made up of xylose and glucuronic acid (Dhepe & Sahu, 2012).

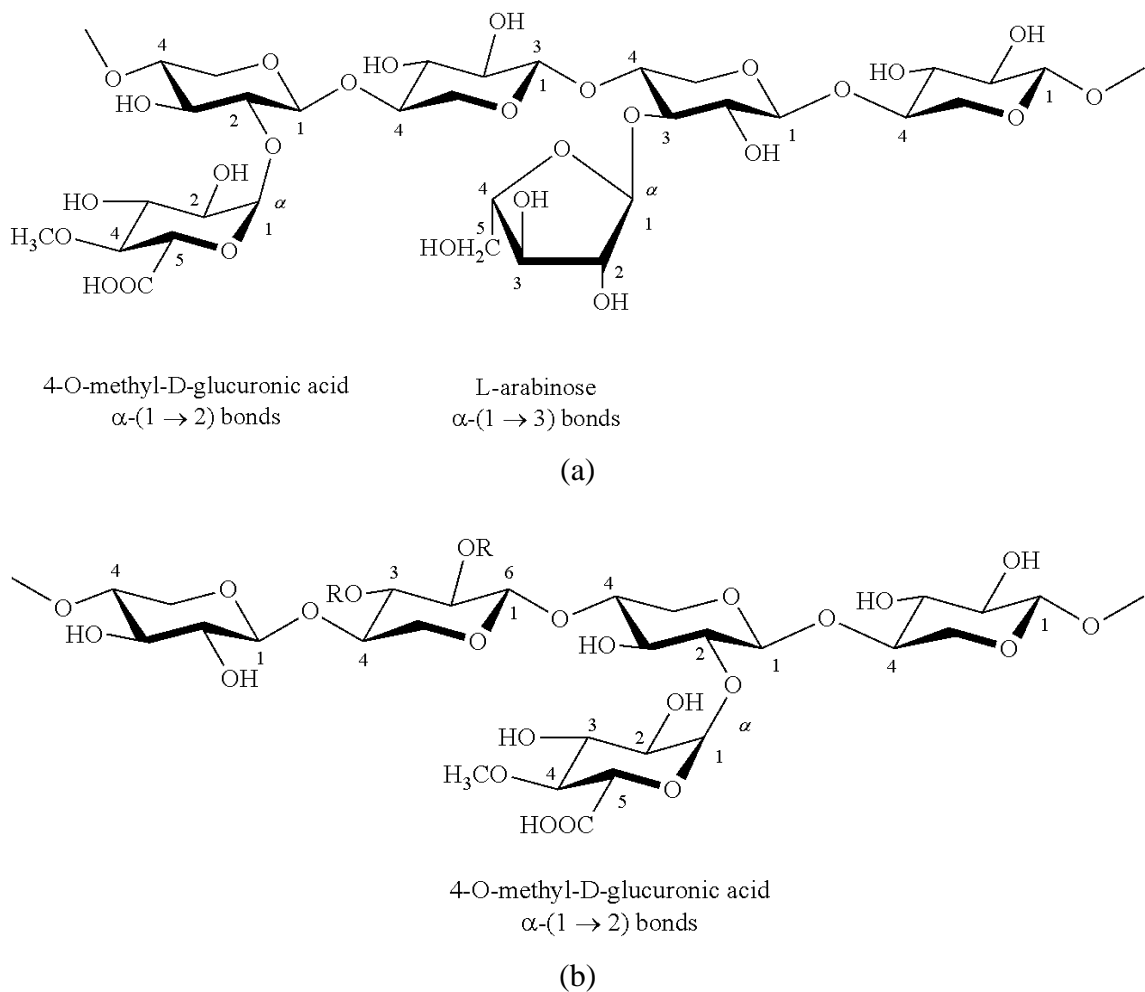


Figure 2-4: Chemical Structure of Hemicellulose: (a) Softwood; (b) Hardwood (Dhepe & Sahu, 2012)

2.3.3 Lignin

Lignin represents the third most abundant organic compound in nature after cellulose and hemicellulose. It is a complex network formed by polymerization of phenyl propane units and constitutes the most abundant non-polysaccharide fraction in lignocelluloses (Sanchez, 2009). Figure 2-5 shows three basic monomers in lignin (p-coumaryl alcohol,

coniferyl alcohol, and sinapyl alcohol) which are linked by alkyl–aryl, alkyl–alkyl and aryl–aryl ether bonds. Lignin acts as cement for the cross-linking between cellulose and hemicellulose to form a rigid three-dimensional structure of the cell wall (Palmqvist & Hahn-Hagerdal, 2000). It is also water insoluble and optically inert. These properties of lignin make it the most recalcitrant component of the plant cell wall in which the higher the lignin content, the greater the resistance of the biomass to chemical and biological degradation. It becomes a major barrier for utilization of lignocellulosic biomass in bioconversion processes. Furthermore, lignin is thermally stable over a wide temperature range of 100–900 °C depending on the precursors of the lignin (Yang *et al.*, 2007). Thus, lignin remains the less modified component among other polymers and a biomass with higher lignin content is expected to yield more solid products.

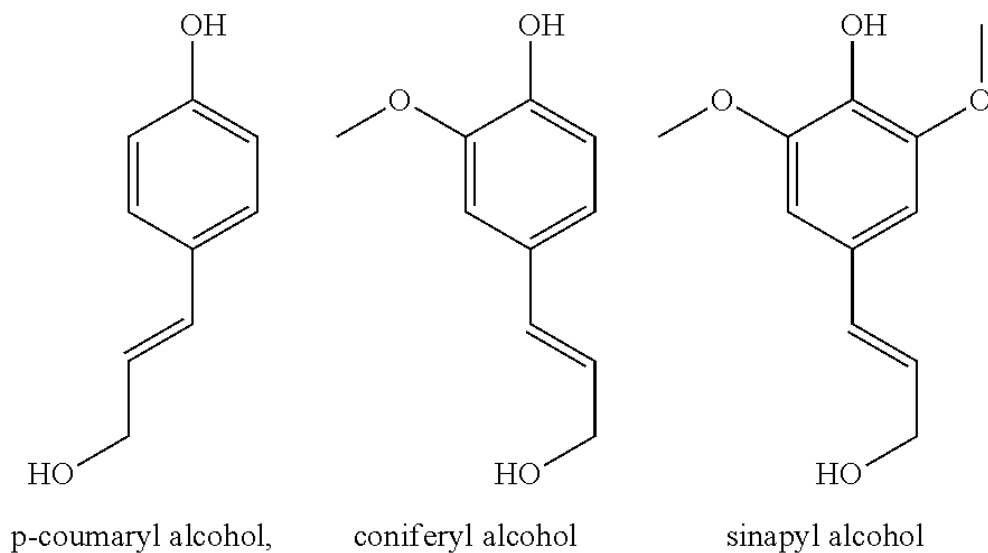


Figure 2-5: Three basic monomers of lignin (Albizati & Tracewell, 2012)

2.4 Palm oil and Oil Palm Biomass in Malaysia

Oil palm tree (*Elaeis guineensis*) originated from the tropical rainforests of West and Southwest Africa. It was first introduced to Malaysia in 1870 through the Singapore Botanic Gardens as an ornamental plant (Mohammed *et al.*, 2011). Once its commercial value was recognized, the oil palm trees were grown in plantation on large scale. The tree bears fruit at the age of about two to three years. However, maximum yield can only be achieved in the age of about 12 to 14 years, which then continuously declines until the end of its economic life at 25 years old (Abdullah, 2003). It takes about five to six months to develop from pollination to maturity before it can be harvested. The fruits are developed in large condensed infructescence which is often called fresh fruit

bunches (FFB). The fruit which is rich in oil comprises a soft oily pulp (mesocarp) with a single seed (palm kernel) inside. The oil extracted from the pulp of the fruit is usually made into edible oil while the kernel is used mainly for soap manufacturing.

Palm oil is considered the world's largest source of oils and fats with 56.1 million tonnes (31.3%) of the world's total oils and fats output (Sime Darby, 2014). Consequently, oil palm is recognized as a major economic crop which has triggered the expansion of plantation area in Malaysia. Malaysia as a tropical region has also flavoured the development of oil palm cultivation. As the second largest oil palm-producing country that comes after Indonesia, Malaysia accounts for 39% of world's palm oil production and 44% of world's exports (MPOC, 2009). In 2012, Malaysia has produced 18.79 million ton of crude palm oil (CPO) as shown in Figure 2-6.

Each year, there is an increase in the amount of oil palm biomass wastes. In 2010, the oil palm biomass solid wastes accounted for 80 million tonnes of dry biomass and it is expected to rise to 100 million dry tonnes by the year 2020 (AIM, 2011). Oil palm biomass can be derived from different sources of production sites as shown in Figure 2-7. In term of land use, Malaysia had reached 5.08 million hectares of oil palm plantation in 2012, that increased by 11.8% in comparison with 2008 as shown in Figure 2-6. This large plantation area generated a vast amount of waste in the form of fronds and trunks. Most of these wastes are usually left to rot for soil regeneration or burnt on the plantation site. However, the Department of Environment has discouraged burning of these materials due to pollution and possible forest burning problems (Sopian *et al.*, 2000). This large volume and type of oil palm residues are also expected to rapidly increase and will become a serious problem in the future. Hence, the best solution is to minimize and recycle the waste, and recover the energy as much as possible for further utilizations such as combustion, gasification and co-firing.

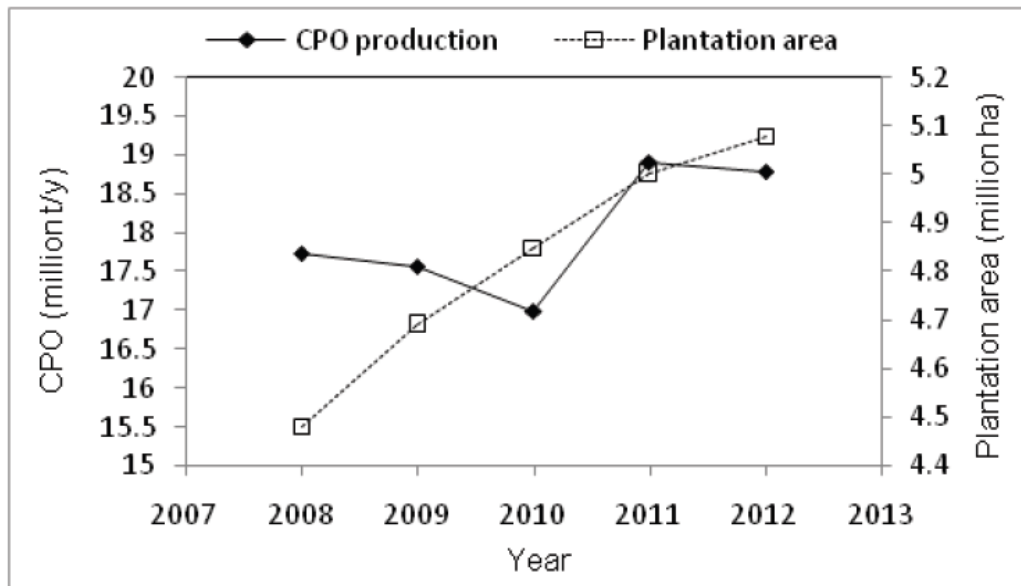


Figure 2-6: Crude palm oil (CPO) production and plantation area in Malaysia (Aljuboori, n.d.)

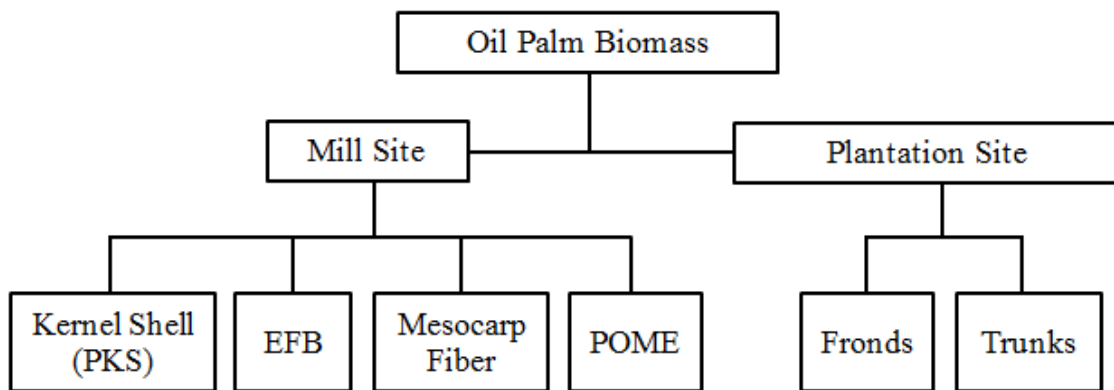


Figure 2-7: Oil palm biomass residue and source of generation

2.4.1 Oil Palm Fronds (OPF)

Oil palm frond (OPF) is the most abundant type of oil palm waste. They are largely available during felling operations and pruning during fruit harvesting. However, at present OPF is not given much attention unlike the other types of biomass produced by oil palm tree. Other than being utilized as ruminant feedstock, they are often dumped at the plantation site for soil conservation, erosion control and ultimately the long-term benefit of nutrient recycling (Zahari *et al.*, 2003). Efforts in studying oil palm frond gasification based on experiment approach was reported by Atnaw *et al.* (2011), bearing a potential result where OPF might be a prospective biomass fuel for heat and energy generation. Hence, there is an opportunity to utilize OPF for biomass energy generation

due to its abundant supply and considerable energy content. Furthermore, OPF is a lignocellulosic material available at a very low cost which would represent a valuable renewable source of various products and chemicals (Goh *et al.*, 2010a). Table 2-3 shows some chemical contents of lignocellulosic OPF.

Table 2-3: Chemical compositions of OPF

Components	Abnisa <i>et al.</i> (2013)	Wanrosli <i>et al.</i> (2007)
Cellulose (%)	50.33	47.60
Hemicellulose (%)	23.18	34.60
Lignin (%)	21.70	15.20
Ash (%)	0.24	0.70

2.4.2 Oil Palm Trunks (OPT)

The average economic life-span of oil palm trees is usually about 25 years due to decreasing yield or increasing height which causes harvesting difficulty. There is a large quantity of cellulosic raw material generated in the form of felled trunks during replanting activities and it contributes a large amount of agricultural waste in Malaysia. Oil palm tree is around 7-13 m in height and 45-65 cm in diameter, measuring 1.5 m above the ground level (Khalil *et al.*, 2010). The OPT has a number of potential uses such as lumber, pulp and paper, reconstituted boards, bio-composites, animal feed, and fuel (Mokhtar *et al.*, 2008).

However, in most of the practices, oil palm trunks are shredded after felled, and are disposed by burning or leaving them on the ground to rot. Both processes have disadvantages in term of environmental sustainability. Burning leads to air pollution and it takes more than 1 year for them to completely decompose, which can hinder the replanting process (H'ng *et al.*, 2011). To overcome this problem meanwhile applying zero waste management solution, utilization of OPT as biomass feedstock will be a solution approach for making use of these abundant waste. Like other wood-based biomass materials, OPT is also rich in its lignocellulosic content as shown in in Table 2-4.

Table 2-4: Chemical compositions of OPT

Components	Ezebor <i>et al.</i> (2014)	Lamaming <i>et al.</i> (2014)	Basyaruddin <i>et al.</i> (2012)
Cellulose (%)	42.29	41.18	44.40
Hemicellulose (%)	30.06	31.42	29.30
Lignin (%)	21.37	19.19	21.20
Ash (%)	1.48	2.49	1.50

2.5 Biomass Conversion Methods

The use of fossil fuels could hardly be shifted to biomass for energy generation due to the bulky and inconvenient form of biomass. Raw biomass which often presents in solid form, cannot be handled, stored, or transported easily (Basu, 2010). Therefore, it is necessary to review other methods of biomass conversion before proceeding to the main concerned of the study, which is the torrefaction process. Unlike torrefaction process, methods like fermentation, gasification, and pyrolysis mainly focus on the conversion of solid biomass into liquid or gaseous fuels. There are also other methods that can convert raw biomass into sources of power, heat, and fuels for potential use. These biomass conversion methods can be sorted into two major paths as shown in Figure 2-8.

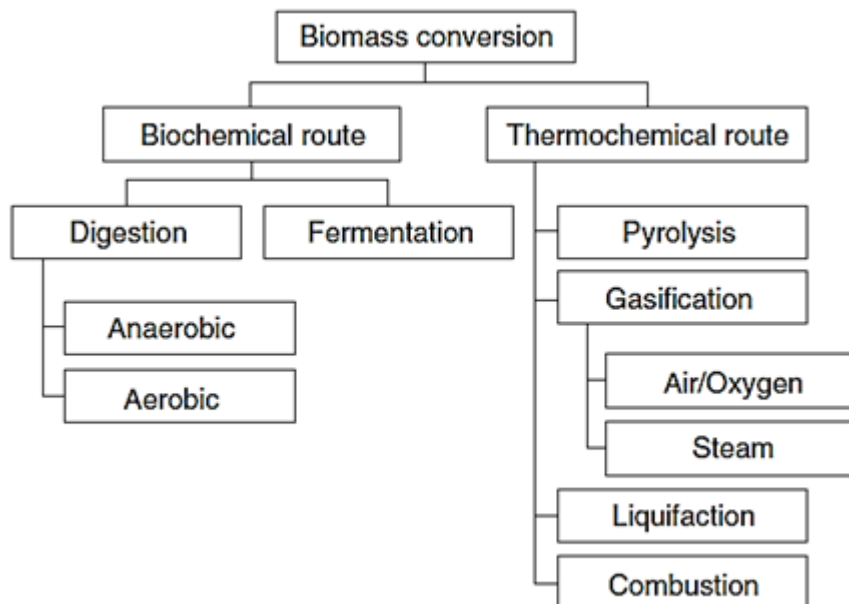


Figure 2-8: Biomass conversion methods in two major paths (Basu, 2010)

2.5.1 Biochemical Conversions

Biochemical conversions involve various chemical reactions catalytically mediated inside microorganisms as whole-cell biocatalysts or enzymes to convert fermentable biomass substrates into fuels or other high-value commodities (Balat, 2011). Biochemical conversions are among the most promising, environmentally sustainable alternatives for reducing atmospheric carbon dioxide levels. Despite of their environmentally friendly manner in which fuels can be produced without pollutants, biochemical conversions takes much longer time compared to rapid thermochemical reactions (Srirangan *et al.*, 2012). However, they do not require much energy such as external heat source which thermochemical conversions do. Biochemical conversions aim to transform biomass into usable products such as gas (methane and carbon dioxide) and waste (fertilizer) with a little water by using microorganisms. The biochemical process mostly refers to anaerobic fermentation with increasingly interest among the researchers nowadays.

Anaerobic fermentation is mainly used to produce biogas. Anaerobic fermentation of biomass involves four key of biological and chemical stages: hydrolysis, acidogenesis, acetogenesis, and methanogenesis. The terminal stage for anaerobic fermentation, methanogenesis plays a significant role in converting biomass into biogas. This biogas normally consists 60-70% of methane, 20-40% of carbon dioxide and negligible amount of water (Srirangan *et al.*, 2012). The production of methane and carbon dioxide through methanogenesis process is highly dependent on external factors especially the pH condition. Methanogenesis is favourable in the pH range between 6.5 and 8. The crude biogas from anaerobic digestion has a considerable heating value of about 26 MJ/m³ and it is an inexpensive energy source that can be burned for heat generation (Kucuk & Dermirbas, 1997). Besides, purified methane which is compatible to natural gas, is applicable directly as transportation fuel. In addition, anaerobic fermentation also produces indigestible materials in solid and liquid forms called digestate which can be utilized for soil nutritional purpose (Braber, 1995).

2.5.2 Thermochemical Conversions

Thermochemical conversion processes basically involve high temperature treatment to promote structural degradation of lignocellulosic biomass. There are four main thermochemical treatment paths for biomass which include pyrolysis, gasification,

combustion and liquefaction. Table 2-5 generally compares the differences between these conversion processes in terms of temperature range, pressure applied, presence of catalyst, and the need of drying. Further reviews on the four major thermochemical conversions are presented in the following subchapters.

Table 2-5: Comparison in four main thermochemical treatment processes (Demirbas, 2009)

Process	Temperature (°C)	Pressure (MPa)	Catalyst	Drying
Liquefaction	250–330	5–20	Essential	Not required
Pyrolysis	380–530	0.1–0.5	Not required	Necessary
Combustion	700–1400	> 0.1	Not required	Not essential, but may help
Gasification	500–1300	> 0.1	Not essential	Necessary

2.5.2.1 Combustion

Combustion, which refers to burning of biomass in oxidative environment, is one of the traditional methods for heat and electricity generation. Presently, different combustion systems, such as grate boilers and underfeed stokers, are available for the production of heat for large-scale industrial use (100–3000 MW) or for district heating (<100 MW) (Srirangan *et al.*, 2012). Besides, cogeneration systems are also available through the use of steam turbines. In more advanced technologies such as fluidized bed combustion system, power generation efficacy can be greatly improved with reduced emissions and increased tolerance in different types of biomass (Demirbas, 2001). However, these technologies are currently not economically feasible as it involves in the distribution networks and processing of biomass with high moisture content. Biomass is used either as a standalone fuel or as a supplement to fossil fuels in a boiler. The latter option, which is often called co-combustion or co-firing, is commonly applied as the fastest and least-expensive means for decreasing the emission of carbon dioxide from an existing fossil fuel plant (Basu, 2010).

2.5.2.2 Pyrolysis

Pyrolysis is a thermal conversion for biomass degradation without the presence of oxygen in a temperature scope from 350°C to more than 800°C (Balat *et al.*, 2009). Torrefaction is also a form of pyrolysis, but with a lower range of temperature from about 200°C to 300°C. Pyrolysis can be divided into three variations: mild pyrolysis

(torrefaction), slow pyrolysis, and fast pyrolysis, depending on the operation parameters such as temperature, particle size, temperature, and residence time. Slow pyrolysis of wood is used to produce charcoal while fast pyrolysis is applied for production of liquid fuel (bio-oil) (Basu, 2010). Figure 2-9 illustrates the pyrolysis process occurring in a biomass particle. The initial product of pyrolysis process consists of solid char and condensable gases. This condensable gas further breaks down into non-condensable gases (CO, CO₂, H₂, and CH₄), liquid, and char. The biomass char has a heating value at about 32 MJ/kg, which is substantially higher than the untreated biomass (19.5-21 MJ/kg) and its liquid product (13-18 MJ/kg) while the gases constitute a heating value of 20 MJ/Nm³ (Diebold & Bridgwater, 1997).

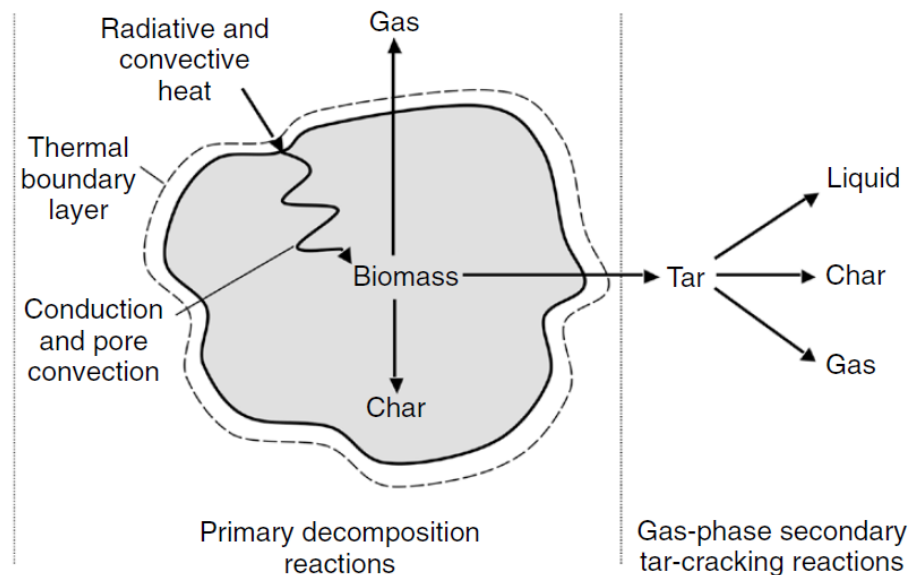


Figure 2-9: Pyrolysis of a biomass particle (Basu, 2010)

2.5.2.3 Gasification

Gasification is an efficient means of converting low-value fuels and residues into a synthesis gas (syngas). Unlike pyrolysis, gasification involves a controlled amount of oxygen to convert carbonaceous material such as lignocellulosic biomass into permanent gases (CO, CO₂, H₂ and CH₄) at high temperature range of 700–1000°C (Mohammed *et al.*, 2011). Three oxidants are commonly used in gasifiers: air, pure oxygen, steam, or a mixture of these. A major disadvantage of air-blown gasification is that atmospheric nitrogen acts as a diluent which reduces the syngas heating value. Nipattummakul *et al.* (2010) reported that steam gasification could increase the hydrogen yield thrice as compared to air gasification. However, the operational cost is a

major problem due to demand for an external heat source for steam production. On the other hand, use of oxygen as gasifying agent contributes to a syngas with intermediate heating value and is generally the cleanest syngas with regard to tars but it leads to simultaneous problem of cost and safety as it requires a pure oxygen supply. The major concerns in the application of gasification is that tars, heavy metals, halogens and alkaline compounds are released within the product gas, which can cause environmental and operational problems. Thus, the key of gasification is often referred to achieving cost efficient and clean energy recovery from biomass solid wastes to curb the problems associated with the release and formation of these contaminants.

2.5.2.4 Liquefaction

Liquefaction of solid biomass can be addressed through pyrolysis and gasification processes as discussed before, as well as via hydrothermal process. Hydrothermal liquefaction of biomass provides a direct pathway for liquid biocrude production by contacting the biomass with water at elevated temperatures (300–350 °C) with high pressure (12–20 MPa) for a period of time (Basu, 2010). Water plays a crucial role as it acts as a reactant and catalyst simultaneously throughout the hydrothermal liquefaction process. Low viscosity and high solubility of organic molecules from biomass make subcritical water an excellent medium for fast, homogeneous and efficient reactions (Toor *et al.*, 2011). However, corrosion is the major problem due to the relatively dense and polar character of subcritical water environment. The processing option is particularly applicable to wet biomass feedstocks which subsequently eliminate the need to expend energy to dry the feed before processing, as required in other thermochemical conversion processes such as pyrolysis and gasification.

2.6 Torrefaction

Torrefaction, often known as a mild pyrolysis process, is carried out under atmospheric pressure in a narrow temperature range from 200°C to 300°C without the presence of oxygen (Clausen *et al.*, 2010). The process is characterized with a heating rate lower than 50°C/min and a residence time less than 1 hour (Chen & Kuo, 2010). This thermal pretreatment of biomass will result in three main products such as dark colour solid products, yellowish colour acidic aqueous products, and non-condensable gaseous products (Deng *et al.* 2009). Unlike pyrolysis which focuses more on its volatile

products, the major motivation of torrefaction is to maximize the solid yield. During the process, the raw biomass encounters three major reactions which include decomposition, devolatilization and depolymerisation. These processes cause raw biomass loses most of its moisture and the biopolymers (cellulose, hemicellulose and lignin) partly decompose, giving off various type superfluous volatiles with low heating value (Fauzianto, 2014). The final product is the remaining solid, dried, and blackened material, namely torrefied biomass.

The advantages of torrefaction are significant in the way of improving the physical characteristics of biomass. The torrefaction process which depends on its severity, fibrous, tenacious and hydrophilic properties of biomass can be altered, leaving a more favourable homogenous solid fuel with hydrophobic property and increased calorific value. These behavioural changes can have significant advantages in the supply chain, since logistics can be made simpler, more cost effective and compatible with coal. The hydrophobic characteristic prevents torrefied biomass to exhibit biodegradation such as mould and rotting, thus allowing storage of torrefied biomass to be more attractive than non-torrefied biomass. Also, biomass torrefaction will partly devolatilize leading to a decrease in mass, but increase of energy density in the solid product which makes it more attractive for transportation.

However, there are still some disadvantages of torrefaction process. Despite higher calorific value can be achieved after the process, the initial energy content of the torrefied biomass is only preserved and yet not improved significantly (Van Der Stelt *et al.*, 2011). Although torrefaction process is able to enhance the quality of untreated biomass, severe mass loss is still a concern as it affects the mass and energy yields of the process. According to Sabil *et al.* (2013), it is suggested to maintain the mass loss of the torrefied materials lower than 50% to ensure the economics of the process. Other than that, there is still limited knowledge on torrefaction process such as process performance, properties of torrefied products, and composition of volatiles.

2.6.1 Mechanism of Torrefaction

In torrefaction process, the physical changes in the biomass can be predicted mainly by understanding the behaviour of the three polymeric constituents. Hemicellulose, which is a highly reactive component of biomass, undergoes decomposition and

devolatilization that contributes a dominant portion of weight loss in torrefaction process (Basu, 2010). Methanol and acetic acid from methoxy- and acetoxy-groups are the major constituents of volatiles gases released during the thermal degradation of hemicellulose (Prins *et al.*, 2006). Therefore, biomass with high content of hemicellulose will result in lower solid product yield compared to biomass with low hemicellulose. Unlike hemicellulose, cellulose shows limited degradation that only starts when approaching 250°C. Despite an insignificant amount of the cellulose degrades within the scope of 200-300°C, water vapour and acids released from hemicellulose may aid in destruction and degradation of cellulose (Nhuchhen *et al.*, 2014). Lignin, with the most carbon content compared to cellulose and hemicellulose, is thermally more stable. Hence, it is relatively higher in composition in the final solid product that leads to an energy dense product after torrefaction. Figure 2-10 shows the weight loss behaviour of cellulose, hemicellulose, and lignin during torrefaction process.

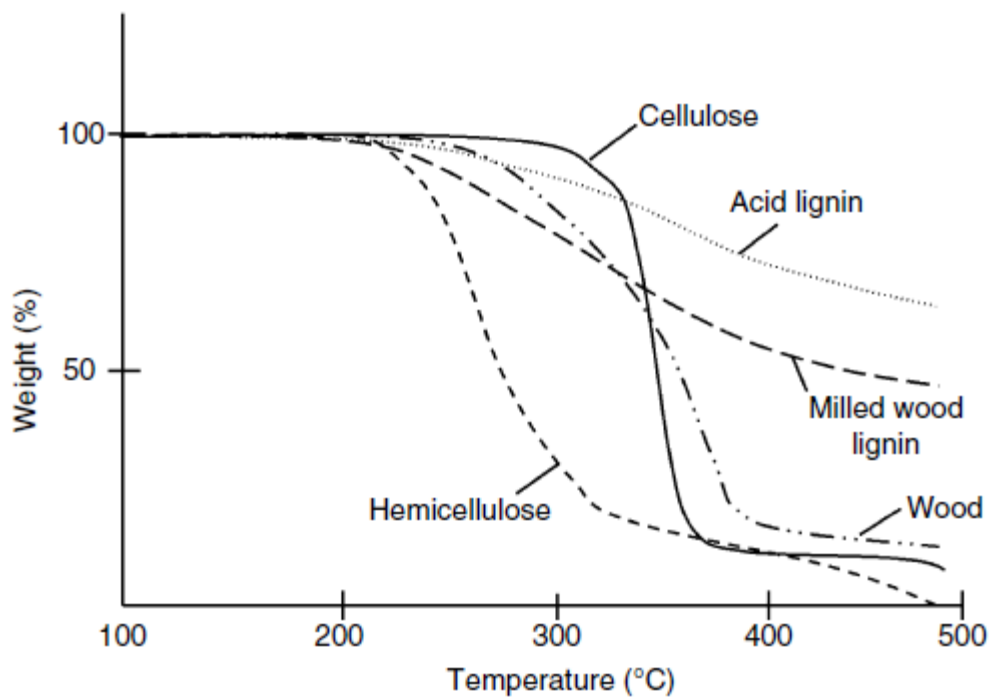


Figure 2-10: Weight loss in terms of cellulose, hemicellulose, and lignin (Basu, 2010)

2.6.2 Effect of Operating Parameters

The following subchapters briefly discuss about the effect of various operating parameters on the torrefaction process. There are four main parameters on torrefaction process which consist of temperature, residence time, particle size, and oxygen content.

2.6.2.1 Temperature

According to Chen & Kuo (2010), torrefaction can be classified into three types such as light, mild, and severe torrefaction depending on the temperature at about 230°C, 260°C, and 290°C respectively. In torrefaction process, temperature contributes a dominant influence on the quality of the torrefied. For instant, a research done by Wannapeera *et al.* (2011), showing that the solid yield decreased from 91.0% to 54.5% when the torrefaction temperature was increased from 200°C to 275°C. On the other hand, Acharya (2013) reported a decrease in energy yield but increase in energy density in torrefaction of Oats when temperature was increased from 210°C to 300°C.

In most of the cases, mass loss or solid yield at different torrefaction temperature can be explained by decomposition and devolatilization of polymeric components of lignocellulosic biomass. Table 2-6 represents the temperature ranges in which thermal degradation of cellulose, hemicellulose, and lignin takes place during pyrolysis process. It can be seen that lignin decomposes over a wider range of temperature compared to cellulose and hemicellulose. Its stability is due to thermal stability of its functional groups containing oxygen (Brebú & Vasile, 2010).

On the other hand, hemicellulose presents to be a highly sensitive polymer in a narrow temperature range. Thus the mass loss during torrefaction is highly dependent on devolatilization of hemicellulose. Unlike hemicellulose, cellulose is relatively more stable in torrefaction process due to its crystalline structure containing strong inter-molecular and intra-molecular hydrogen bonds. Hence, decomposition of cellulose occurs at temperature higher than cellulose does. Typical mass loss percentages of these three polymeric components at different torrefaction temperatures are shown in Table 2-7.

Table 2-6: Temperature range for thermal degradation of cellulose, hemicellulose and lignin

Degradation temperature range (°C)			Source
Cellulose	Hemicellulose	Lignin	
327-407	227-327	127-447	Giudicianni <i>et al.</i> (2013)
315-400	220-315	160-900	Yang <i>et al.</i> (2007)
275-400	200-400	200-500	Sorum <i>et al.</i> (2001)

Table 2-7: Mass loss in polymeric components at different temperatures (Chen & Kuo, 2011)

Temperature (°C)	Cellulose (wt%)	Hemicellulose (wt%)	Lignin (wt%)
230	1.05	2.74	1.45
260	4.43	37.98	3.12
290	44.82	58.33	6.97

2.6.2.2 Residence Time

The net effect of residence time is not significant as compared to the operating temperature in torrefaction process. However, it does influence the torrefied product at a much higher residence time. According to Chen *et al.* (2011), when the residence time is increased, mass loss will also increase which results in lower solid yield. This is mainly due to an increase in the extent of devolatilization (Prins *et al.*, 2006). Condensable product contributes a dominant mass loss at longer residence time as shown in Figure 2-11. Moreover, loss in relative amount of carbon and oxygen contents also increases with the residence time. For instant, about 11% of carbon and 40% of oxygen lost in 15 minutes compared to 26% and 69% in 40 minutes, resulting in more carbon loss per unit of oxygen loss (from 0.28 to 0.38) (Bates & Ghoniem, 2012). As a result, the rate of deoxygenation of biomass slows down at higher residence time, which increases the carbon content in the volatiles generated.

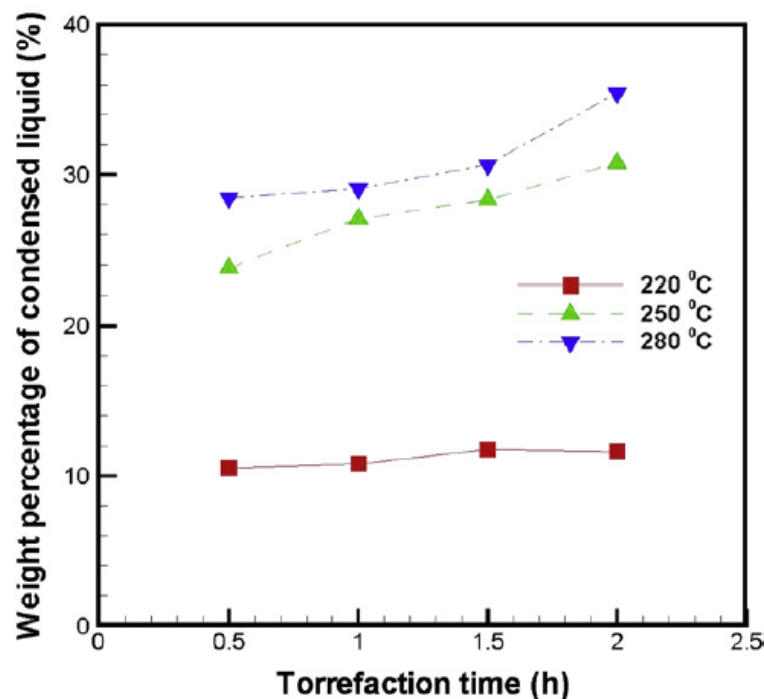


Figure 2-11: Weight loss of condensed liquid with residence time (Chen *et al.*, 2011)

2.6.2.3 Particle Size

Torrefaction process requires certain amount of heat source to preheat, dry, and devolatilize the biomass depending on the size, shape, and properties of biomass. These parameters must be considered as they affect both conductive and convective heat transfer rate from the reactor to the biomass and within the biomass, respectively. A larger piece of biomass contributes to lower surface area per unit mass, resulting in lower convective heat transfer rate. Due to anisotropic and heterogeneous properties of biomass, large particle may encounter non-uniform heat distribution (Nhuchhen *et al.*, 2014). Other than that, the larger particle will result in higher mass transfer resistance that as well slows down the rate of diffusion of volatiles through the particle itself. Peng *et al.* (2012) in the study of torrefaction noted that mass loss in smaller size particles is higher than that of the larger particles due to both higher heat transfer rate and lower resistance to diffusion of volatiles in small particles. Even in a microwave-assisted torrefaction process, Wang *et al.* (2012) also found higher mass loss in finer particle size. Thus, the quality and efficiency of the torrefaction process varies with particle sizes.

2.6.2.4 Oxygen Concentration

For a desired torrefaction process, oxygen has to be eliminated as it enhances the combustion reaction which releases carbon into flue gas instead of preserving it in the solid biomass. In addition, oxygen is not favourable in terms of safety operation in torrefaction process because the temperature of product might increase due to combustion (Nhuchhen *et al.*, 2014). So, torrefaction is suggested to be carried out either by indirect heating or a continuous supply of inert gas.

Presence of oxygen in torrefaction process increases the devolatilization reactions resulting in lower solid and energy yield. For instant, a comparative study of torrefaction process in both nitrogen and air media was made by Lu *et al.* (2012), finding that both solid and energy yield were less in air media compared to that in nitrogen. On the other hand, Tumuluru *et al.* (2011) noted a slight increase in the heating value of wheat straw, willow, and red canary grass when the oxygen concentration in the air media decreases. Despite of undesired torrefied product produced, torrefaction under oxidative media could reduce the torrefaction time needed for a targeted mass loss (Wang *et al.*, 2012). Wang *et al.* (2012) also discussed a

possible change in torrefaction design where the flue gas released can be reused as the working media without any significant variation in the product quality.

2.6.3 Effect of Biomass Colour on Calorific Value

As can be seen from previous researches on torrefaction-related works (Kolokolova *et al.*, 2013; Stelte *et al.*, 2011; Singh *et al.*, 2013), the colour of torrefied biomass typically changes from light brown to dark brown (approaches to the colour of coal) with increasing severity of torrefaction treatment. According to Luo (2011), torrefaction temperature has very strong effect on the colour of solid products. The higher the temperature, the darker the product colour. Research done by Stelte *et al.* (2011) on the torrefaction of spruce at 250°C, 275°C, and 300°C resulted in three products of light brown, dark brown, and black colour as shown in Figure 2-12. The colour change is mainly attributed to chemical changes of the lignin, i.e. the formation of chromaphoric groups, mainly the increase of carbonyl groups (Gonzalez-Pena & Hale, 2009).



Figure 2-12: Colour change during torrefaction process (Stelte *et al.*, 2011)

Therefore, the change in torrefied biomass colour can possibly be characterized as one of the parameter to predict the calorific value of torrefied materials. However, it is noted that not every materials contribute to the same colour. For instant, soft untreated lignocellulosic material like rice straw has brighter colour compared to hard untreated lignocellulosic material like palm kernel shell (see Figure 2-13). As mentioned by Gonzalez-Pena & Hale (2009), the difference in biomass colour is mainly due to their different lignocellulosic composition, where chemical changes in lignin content bring the largest effect in this case. Hence, it is important to classify the tested material (i.e. soft or hard lignocellulosic material) before studying the effect of its colour on calorific

value. This part of characterization has not yet been conducted by any other researchers, resulting as one of the novelties of this research work. Also, due to this reason, this characterization is expected to have only rough prediction on the calorific value of torrefied biomass.



Figure 2-13: Colour of lignocellulosic material (a) Soft: rice straw (b) Hard: palm kernel shell (PKS)

2.7 Summary

In this chapter, review on the use of lignocellulosic materials as biomass energy feedstock has provided an insight on its potential as a candidate for various energy conversion technologies. In addition, a brief discussion on the impacts of different operating parameters towards torrefaction behaviour is also presented and all these considerations give us an idea as well as guidelines to conduct the experiment in a more efficient way. A discussion on the calorific value prediction based on colour of biomass is justified as well. Furthermore, these literature reviews will aid by giving a better concept and understanding towards the results obtained, thus discussion part can be easily coped with.

3 MATERIALS AND METHODS

3.1 Overview

This chapter will discuss the material and methodology applied for this study. A general description on the raw material and chemical used for the experimental study is presented. The methods and measurements implemented in this research will be covered as well in this chapter.

3.2 Raw Materials

The raw biomass materials used in this study included oil palm fronds (OPF) and oil palm trunks (OPT). Fresh oil palm fronds were collected at LCSB Lepar Oil Palm Mill near Gambang, Pahang while oil palm trunk fibres were purchased from Regalis Asia Sdn Bhd located in Kuala Lumpur. The raw materials obtained were further processed to generate OPF and OPT in fibrous form for experimental purpose.

Newly pruned and green oil palm fronds used for the study were collected from LCSB Lepar Oil Palm Mill located in Gambang, Pahang, Malaysia. The petioles of oil palm fronds were used after removing the leaflets. The petioles were washed with tap water to remove unwanted dirt, soil, dust, and insects. They were then processed using press machine to produce oil palm frond fibres as shown in Figure 3-1. The oil palm frond fibres produced were then dried under sunlight for 3 days.

Both oil palm frond and trunk fibres were cut into smaller form with a diameter of 1 mm and a length of 10 mm for experimental purpose as can be seen in Figure 3-2. Subsequently, the samples were placed in sealed polyethene bags and stored indoor at room temperature until experiments were carried out.



Figure 3-1: OPF fibres produced from press machine

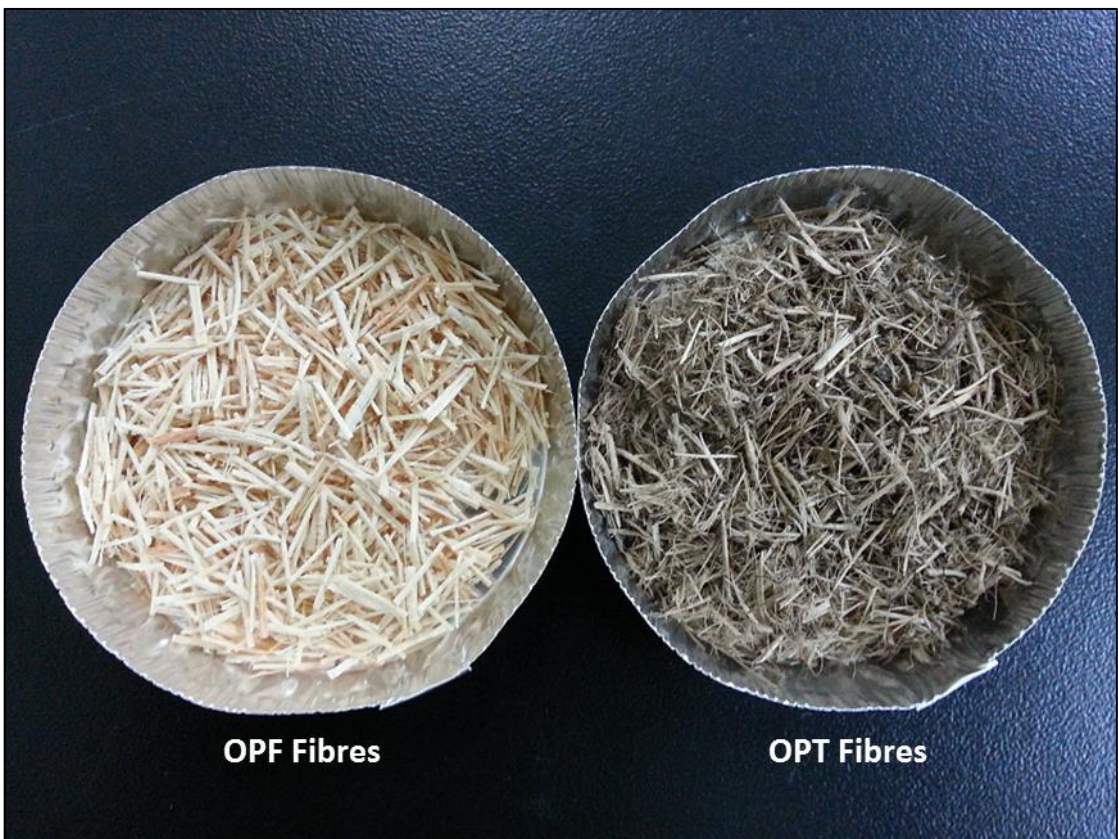


Figure 3-2: OPF and OPT fibres in desired size

3.3 Chemical

The only chemical involved in the whole study of torrefaction process is nitrogen gas. The nitrogen gas from the compressed nitrogen cylinder supplied by Air Product and Chemicals Inc. is located in UMP FKKSA Lab. The nitrogen tank used consists of a compressed nitrogen cylinder and a gas regulator together with a pressure gauge. During the torrefaction process, nitrogen gas is purge at 1 atm to ensure an inert atmospheric condition by eliminating the oxygen from the torrefaction reactor.

3.4 Torrefaction Process

A vertical reactor used for the torrefaction process was a stainless steel (Grade 304) seamless tube with an internal diameter of 16.0 mm and a length of 490 mm. A ring was originally fixed and located 160 mm measured from the bottom of the reactor which acted as a support for biomass sample. The reactor and its support ring are shown in Figure 3-3 below.



Figure 3-3: Stainless steel reactor and its support ring

The experiment was carried out to study the effect of different temperature on the calorific value, mass yield and energy yield. The experiment was started by setting up all the parameters studied in the experiment at the control system of the pyrolyzer. A total of three temperature patterns were set at 200°C, 250°C, and 300°C. In each case a small amount of glass wool was placed above the ring to prevent biomass sample from leaking during the torrefaction process. Then a prescribed amount (10 grams) of biomass sample in fibrous form was weighed and inserted in the reactor. Nitrogen gas at a pressure of 1 atm was then flushed into the reactor for 15 minutes in order to eliminate the oxygen inside. This was followed by selecting the required pattern which was first at

temperature of 200°C with a constant heating rate of 10°C/min, heated by an electric furnace surrounding the reactor. During the process, the exit gas was trapped in a cold bath to prevent emission of harmful gas to the atmosphere. After 30 minutes of torrefaction process, the heater was turned off and the reactor was left to cool down to ambient temperature. The torrefied sample was collected, weighed and kept in an air tight sample bottle prior to characterization. The steps above were repeated by changing the temperature pattern at the control system of pyrolyzer to 250°C and 300°C. Each experiment was repeated for 3 times to obtain optimal result. A schematic diagram of experimental setup is shown in Figure 3-4.

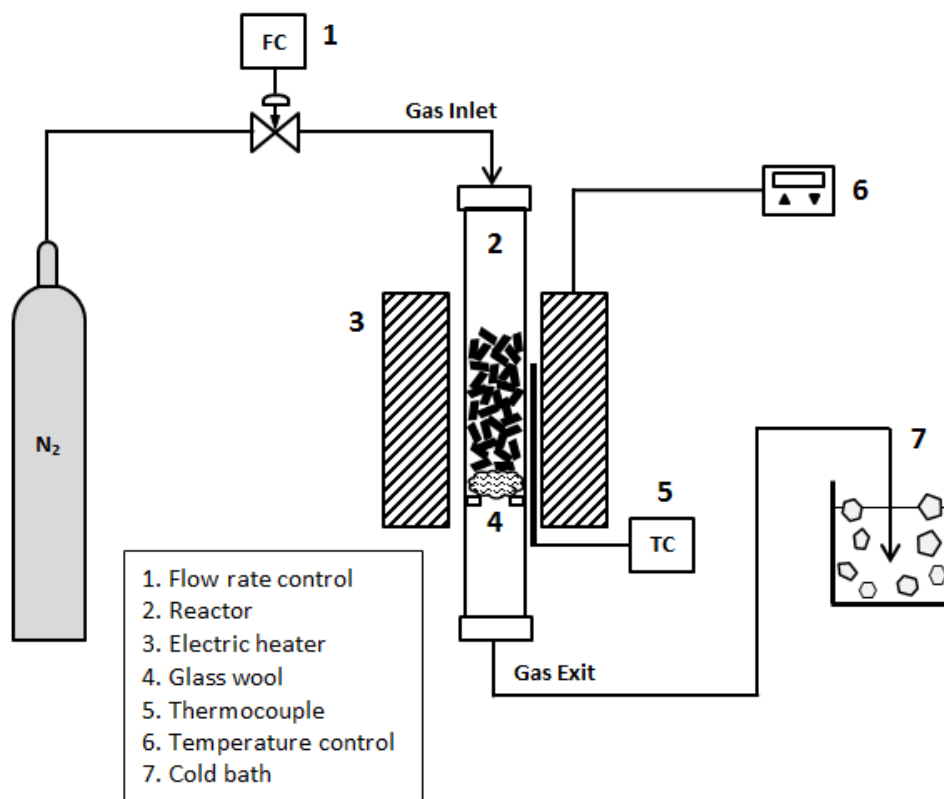


Figure 3-4: Schematic diagram of experimental setup

3.5 Calorific value Prediction using RGB Colour Model

Identification of the calorific value of torrefied biomass is essential to measure its fuel quality. However, calorific value of torrefied biomass needs to be experimentally determined, for example using bomb calorimeter where each run will consume a portion of solid sample for combustion. A possible method to predict the calorific value of a torrefied biomass without the need of conducting bomb calorimeter experiment is by comparing the colour and calorific value of tested biomass with the data from previous

researches (Singh *et al.*, 2013; Luo, 2011; Stelte, 2012; Stelte *et al.*, 2011). The data of colours and calorific values obtained from previous researches on similar torrefaction-related processes are summarized in Appendix A.3.

It is difficult to distinguish the exact colour of an object due to the different ability of the human eye and also, human perception on colour is subjective. To predict the calorific value based on the colour of torrefied material, the colour has to be mathematically presented (i.e. in numbers or values). This section describes the way in which human colour vision can be modelled and calorific value of torrefied material can be mathematically calculated and predicted.

The RGB (Red, Green, Blue) color model is one of the abstract mathematical model that describes the way colours can be represented as tuples of numbers. This model defines a color space in terms of three components:

- i) Red, which ranges from 0-255
- ii) Green, which ranges from 0-255
- iii) Blue, which ranges from 0-255

The colour is expressed as an RGB triplet (R,G,B), each component of which can vary from zero (0) to a defined maximum value (255). If all the components are at zero (0) the result is black, whereas if all are at maximum (255), the result is the brightest representable white. The RGB color model is an additive one. In other words, Red, Green and Blue values (known as the three primary colors) are combined to reproduce other colors. For example, the color "Red" can be represented as [R=255, G=0, B=0], "Violet" as [R=238, G=130, B=238], etc. Its common graphic representation is shown in **Error! Reference source not found.**

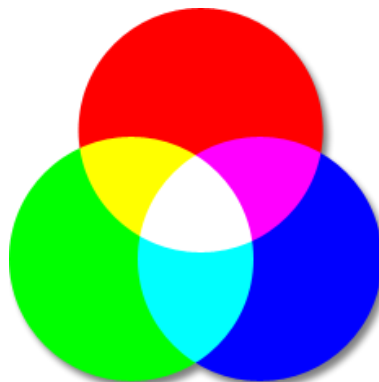


Figure 3-5: RGB colour model

To predict the calorific value of the torrefied OPF and OPT, the RGB index (values of R,G, and B between 0-255) of the tested sample needs to be determined. First, a photo of the torrefied material is taken and the RBD index is determined using computer software, namely Pixeur v3.2 created by Veign (2009) as can be seen in **Error! Reference source not found.**

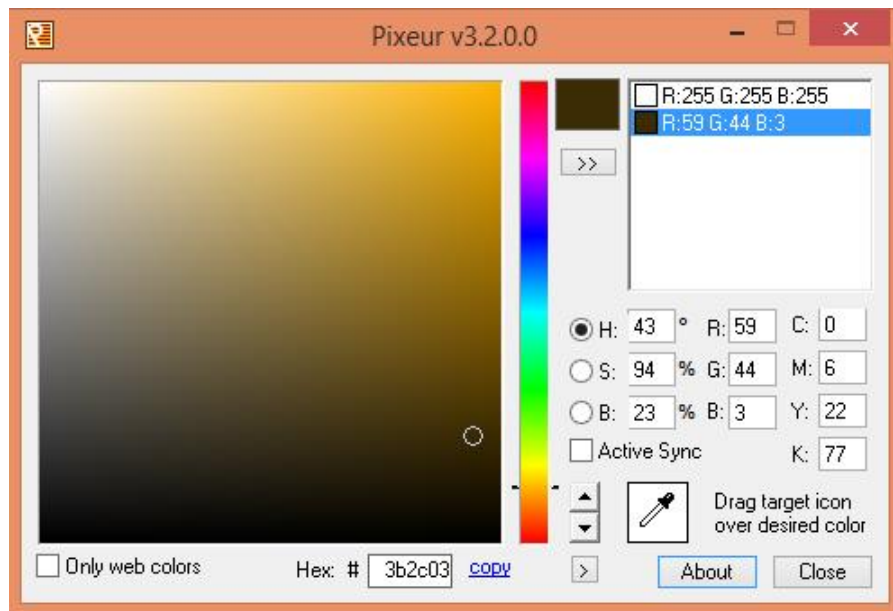


Figure 3-6: Colour picking software – Pixeur v3.2 (Veign, 2009)

Using the data of colours and CVs obtained from the previous studies related to torrefaction of lignocellulosic biomass, a CV predicting tool, namely CV Predictor v1.0 (**Error! Reference source not found.**) is created using Microsoft Excel spreadsheet. The values of RGB index are the only inputs to operate the tool. Detailed steps in developing the CV Predictor v1.0 can be viewed in Appendix A.3.

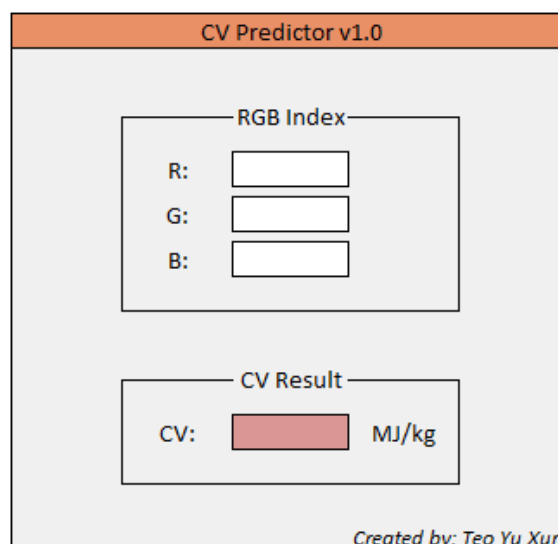


Figure 3-7: CV Predictor created using Microsoft Excel spreadsheet

3.6 Characterizations

Characterizations of moisture content, calorific value, Fourier Transform Infrared (FTIR) Spectrometry, and Thermogravimetric Analysis (TGA) are presented in the following subchapters.

3.6.1 Moisture Content

Moisture content or moisture absorption is one of the important studies in this research as it contributes in determining the hygroscopic property of the biomass before and after torrefaction process. The characterization of moisture content for each of the types of biomass fibres was determined by using the electric oven which was located in the Environmental Engineering Lab of University Malaysia Pahang (UMP).

First, a prescribed amount of samples were placed into the heating boats. The heating boats were then inserted into the electric oven for duration of 24 hours at the temperature of 105°C. The initial weight and the final weight of the samples were determined using analytical balance located in the Environmental Engineering Lab. The readings were recorded and calculation was done to obtain the percentage value of moisture content. The apparatus used are shown in Figure 3-8 and Figure 3-9 below.

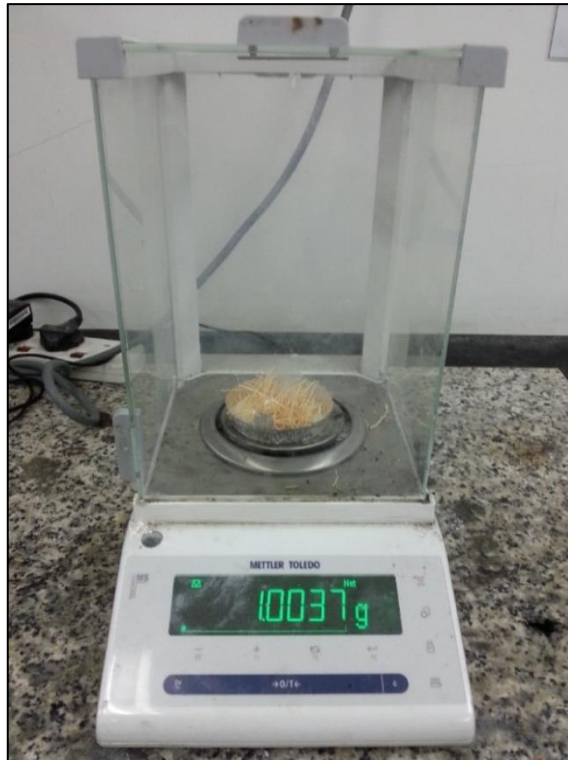


Figure 3-8: Electronic Balance in FKKSA Environmental Engineering Lab



Figure 3-9: Electric Oven in FKKSA Environmental Engineering Lab

Moisture content refers to the amount of water contained in the biomass. It can be given on volumetric or mass (gravimetric) basis. The initial and final weight readings of sample were taken before and after drying in oven at 105°C for 24 hour. In this study,

gravimetric moisture content (MC) is applied and it can be defined mathematically in Eq. (3.1) as proposed by Mohideen *et al.* (2011).

$$MC (\%) = \frac{\text{Initial weight} - \text{Final weight}}{\text{Initial weight}} \times 100 \quad (3.1)$$

3.6.2 Calorific Value

The calorific value of each sample is determined by using the bomb calorimeter which was located at the Basic Engineering Lab of UMP. The steps of determining the calorific value was followed exactly the same experiment of bomb calorimeter carried out in the course of Basic Engineering Lab. The calorific value was measured before and after the torrefaction process for all the biomass samples used in this study. Before starting the experiment using bomb calorimeter, the studied samples were ground using blender and sieved to obtain fine powder samples. This was necessary to ensure good contact between sample and fuse wire in order to provide more accurate reading throughout the bomb calorimeter test.

The experiment was started with the step in which a combustion capsule was being cleaned and dried, meanwhile, 0.5 g of sample was weighed accurately using analytical balance. Then, the sample was filled into the combustion capsule, followed by fixing it on the bomb head. 10 cm of fuse wire was cut and the wire was attached on the bomb head by lifting up the cap, followed by inserting the wire through the eyelet, a “U” shape was made and the cap was pulled downward. The fuse wire was ensured to immerse or touch the sample but it should not touch the combustion capsule to prevent short circuit.

Next, the bomb head was attached carefully with combustion bomb until it is tight. The bomb was then filled with oxygen gas while the oval bucket was filled with 2 L of distilled water accurately. The lifting handle was attached to the two holes in the side of the screw cap and the combustion bomb was lowered into the water. The combustion bomb was handled carefully so the sample will not be disturbed. It was necessary to ensure there was no leaking of bubbles coming out from the combustion bomb. The handle was removed and any drops of water were shaken off back into the bucket. The ignition lead wire was pushed into the terminal sockets on the bomb. The cover was put vertically on the jacket with the thermometer facing toward the front. The stirrer was

turned by hand to ensure that it runs freely before slipping the drive belt onto the pulley and starting the motor. The stirrer was left to run until the thermometer reading reached constant level. After that, the bomb was fired by pressing and holding the ignition button until the indicator light goes out. The temperature was read and recorded at one minute intervals until it reaches constant for at least 3 similar temperature reading.

After the last temperature reading, the motor was stopped, the belt was removed and the cover was lifted from the calorimeter vertically. The cover was then put carefully on the support stand. The ignition leads wire was removed and the bomb was lifted out of the bucket. The bomb was wiped with a clean towel. The knurled knob on the bomb head was opened slowly to release the gas pressure. After releasing all the pressure (no sound), the cap was unscrewed, the head was lifted out of the cylinder and it was placed on the support stand. All the unburned pieces of fuse wire were removed from the bomb electrodes, being straightened and their combined length was measured in centimetre. The steps were repeated three times for each sample to obtain average reading. Figure 3-10 shows the structure of the bomb calorimeter.

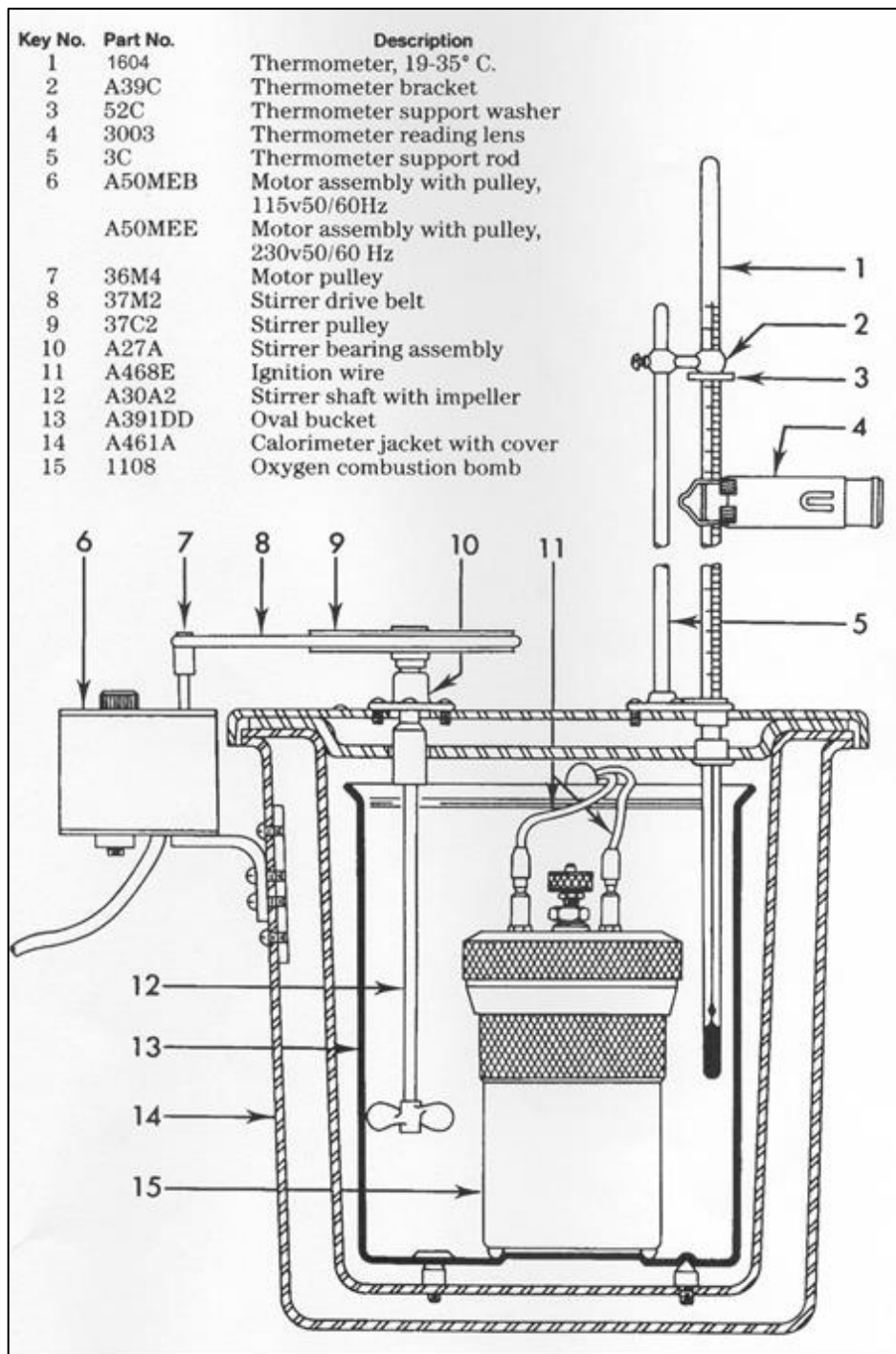


Figure 3-10: Structure of Bomb Calorimeter

The calorific value (CV), also known as higher heating value (HHV), included the latent heat of the vapour emitted from the specimen. The calorific value (CV) was determined based on the length of unburned fuse wire collected in the bomb calorimeter using Eq. (3.2).

$$CV \text{ (cal/g)} = \frac{tW - e_1 - e_2 - e_3}{m} \quad (3.2)$$

where t = temperature rise

$$W = 2409.26 \text{ cal/}^\circ\text{C}$$

e_1 = correction in calories for heat of formation of nitric acid

e_2 = correction in calories for heat of formation of sulfuric acid

e_3 = correction in calories for heat of combustion of fuse wire

$$= 2.3 \times \text{centimeters of fuse wire consumed in firing}$$

m = mass of sample in grams

$$1 \text{ calorie(cal)} = 4.1840 \text{ Joules(J)}$$

3.6.3 Fourier Transform Infrared (FTIR) Spectroscopy

Fourier Transform Infrared (FTIR) Spectroscopy is a preferable method to qualitatively analyse the functional groups of chemical components available in the virgin and torrefied biomass samples. This provides an insight into the effect of torrefaction process on the decomposition of major polymeric constituents (cellulose, hemicellulose, and lignin) of biomass samples. The analysis was conducted using Thermo Scientific FTIR Spectrometer located at the Faculty of Industrial Science and Technology (FIST) of University Malaysia Pahang. Approximately 1.0 g of particles was used, and spectral outputs were recorded in the transmittance mode as a function of wave number in the range of 4000 to 700 cm^{-1} .

3.6.4 Thermogravimetric Analysis (TGA)

Thermogravimetric Analysis (TGA) is a technique in which the mass of the studied material is monitored as a function of temperature or time. The thermogravimetric analyzer was used to examine the physiochemical structure change of the biomass as well as study its trend of decomposition upon thermal treatment. This analysis was carried out for both raw and torrefied biomass with temperature ranges between 25°C to 800°C at a heating rate of 10°C/min in UMP FKKS analytical lab.

3.7 Mass and Energy Yield

The biomass will subject to changes in mass and energy yield during the torrefaction process. Mass and energy yield were calculated using Eq. (3.3), (3.4), and (3.5) as proposed by Bergman et al. (2005).

$$\text{Mass Yield} = \frac{\text{Mass of sample after torrefaction}}{\text{Mass of untreated sample}} \quad (3.3)$$

$$\text{CV Ratio} = \frac{\text{CV of sample after torrefaction}}{\text{CV of untreated sample}} \quad (3.4)$$

$$\text{Energy Yield} = \text{Mass Yield} \times \text{CV Ratio} \quad (3.5)$$

where CV refers to the calorific value.

4 RESULTS AND DISCUSSION

4.1 Overview

This chapter presents the results and discussions for the research work. The results on moisture content, predicted and experimental calorific value, mass and energy yield, FTIR analysis, TG-DTG analysis were presented and discussed in this chapter.

4.2 Preliminary Results on Moisture Content and Calorific Value

Table 4-1: Moisture content (MC) for raw materials

Type of sample	Sample no.	Before oven-dried (g)	After oven-dried (g)	Experimental MC (wt%)	Referenced MC (wt%)	Source
OPF	1	1.0030	0.9323	7.05	4.30	(Lim & Andresen, 2011) (Goh <i>et al.</i> , 2010b)
	2	1.0037	0.9225	8.09	10.26	
	3	1.0045	0.9278	7.64		
			Average	7.59		
OPT	1	1.0021	0.9505	5.15	4.31	(Salim <i>et al.</i> , 2013) (Sulaiman <i>et al.</i> , 2009)
	2	1.0013	0.9532	4.80	9.74	
	3	1.0006	0.9548	4.58		
			Average	4.84		

*Calculated from eq. (3.1) described in chapter 3.

Based on the result in Table 4-1, the average moisture content (MC) obtained for the OPF and OPT after oven-drying at 105°C for 24 hours are 7.59 wt% and 4.84 wt% respectively. These values are observed to be slightly different, but close to the referenced values as can be seen in Table 4-1. This difference can be explained through different preservation methods of the biomass samples. Varies in pre-drying method and storage handling will result in different moisture content of the samples. In this study, the biomass samples were dried under sunlight for 3 days and stored indoor in a sealed polyethene bags. Therefore, it is possible to have variation in moisture content as compared to the referenced values.

Table 4-2: Calorific value for raw materials

Type of sample	Sample no.	Unburned fuse wire (cm)	Experimental CV (MJ/kg)	Referenced CV (MJ/kg)	Source
OPF	1	2.9	16.0727	15.72	(MPOB, 2011)
	2	3.1	16.0689	17.20	(Chavalparit <i>et al.</i> , 2013)
	3	3.0	17.0788	17.28	(Guangul <i>et al.</i> , 2012)
		Average	16.4068	18.40	(Yuliansyah & Hirajima, 2012)
OPT	1	3.2	17.0750	17.27	(UNEP, 2012)
	2	3.0	18.0869	17.47	(MPOB, 2011)
	3	3.4	17.0711	18.30	(Yuliansyah & Hirajima, 2012)
		Average	17.4110	19.26	(Nipattummakul <i>et al.</i> , 2012)

*Calculated from eq. (3.2) described in chapter 3.

As shown in Table 4-2, the average calorific values of OPF and OPT obtained are 16.41 MJ/kg and 17.41 MJ/kg respectively. These experimental values are close to the referenced values (see Table 4-2) obtained from other researchers' works. There are several factors which could affect the bomb calorimeter experiment. These include the mass of sample used, length of fuse wire consumed, and the most determinant factor, the temperature rise. In addition, the amount of oxygen gas charged in the combustion bomb would be another element affecting the final length of the fuse wire which in turn influenced the calorific value obtained. In this experiment, it was noticed that the optimum oxygen pressure to be charged in the combustion bomb is within the range of 15–18 atm to provide a favourable result and any pressure exceeding 20 atm would burn up the entire fuse wire. As a result, the experimental calorific values obtained for OPF and OPT are reasonably accepted which are within the range of referenced values.

4.3 Predicted Calorific Value of Torrefied Biomass based on Colour

A noted change in colour was recorded in the form of RGB colour model (using colour picker – Pixeur v3.2 software) for all the OPF and OPT at different torrefaction conditions. The obtained RGB index of the tested material was used to predict the calorific value using self-developed CV predicting tool, namely CV Predictor v1.0. The changes in the product colour can be seen in Figure 4-1 and Figure 4-2 while the results of RGB index and predicted CV are tabulated in Table 4-3. The predicted calorific values were compared with the experimental calorific values in subchapter 4.4.



Figure 4-1: Raw and torrefied OPF samples



Figure 4-2: Raw and torrefied OPT samples

Table 4-3: Results of RGB index and predicted CV

Sample	Parameter	Raw	200°C	250°C	300°C
OPF	RGB	R: 239	R: 177	R: 98	R: 41
		G: 220	G: 126	B: 59	G: 35
		B: 195	B: 96	B: 39	B: 33
	CV (MJ/kg)	16.7843	18.3861	20.9873	22.7849
OPT	RGB	R: 178	R: 115	R: 75	R: 25
		G: 136	G: 67	G: 50	G: 21
		B: 109	B: 41	B: 42	B: 21
	CV (MJ/kg)	18.1500	20.6143	21.3327	24.7926

4.4 Effect of Temperature on the Calorific Value

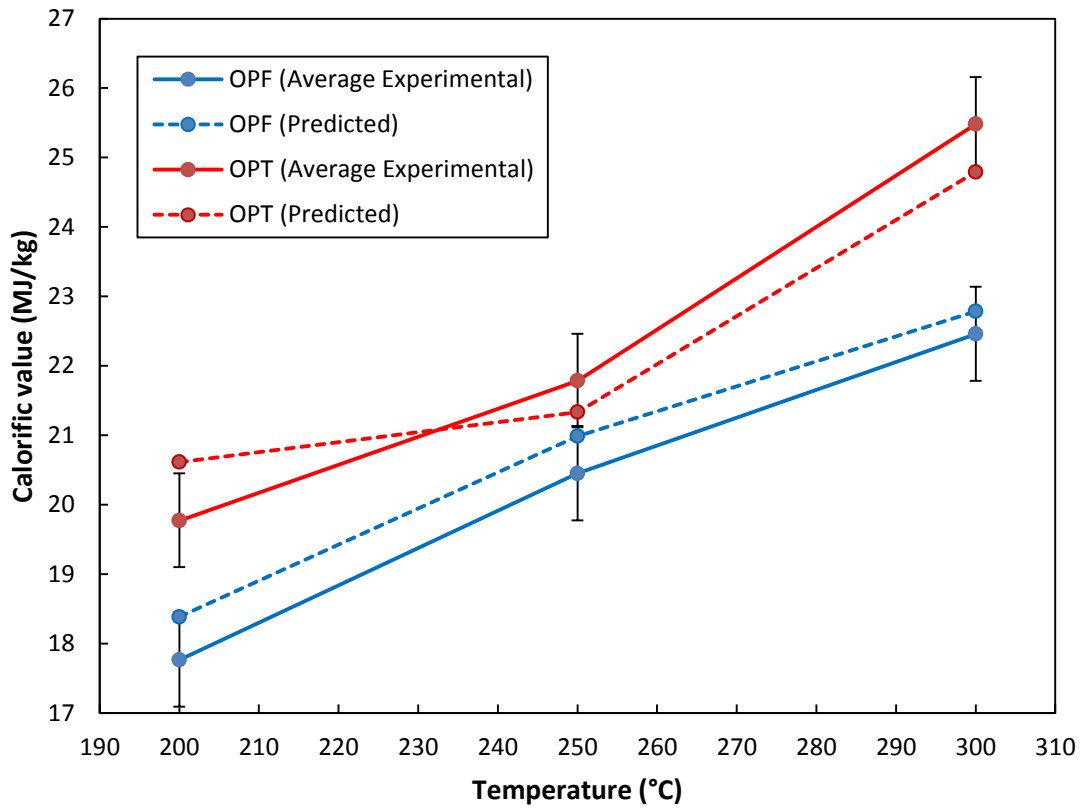


Figure 4-3: Effect of temperature on predicted and average experimental calorific value

Table 4-4: Comparison between experimental and predicted CV

Sample	Condition	Predicted CV (MJ/kg)	Experimental CV (MJ/kg)	Error (%)
OPF	Raw	16.7843	16.4068	2.30
	200°C	18.3861	17.7650	3.50
	250°C	20.9873	20.4511	2.62
	300°C	22.7849	22.4576	1.46
OPT	Raw	18.1500	17.4110	4.24
	200°C	20.6143	19.7714	4.26
	250°C	21.3327	21.7843	-2.07
	300°C	24.7926	25.4823	-2.71

Calorific value (CV) analysis was performed on the biomass samples in both their untreated state and after torrefaction at 200°C, 250°C, and 300°C for a residence time of

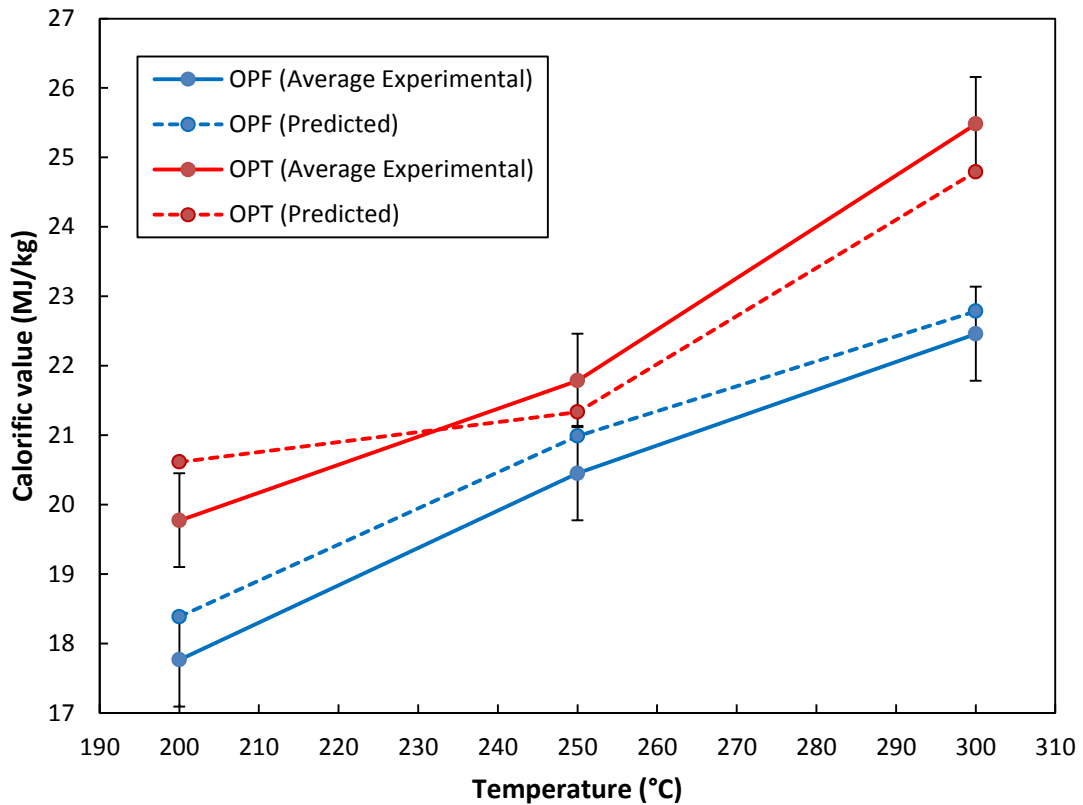


Figure 4-3, the results show that the reaction temperature is a significant variable in the torrefaction of OPF and OPT. For both biomass types, increasing the severity of the torrefaction temperatures caused an increment on the calorific value. The CV of raw OPT is higher than OPF at 17.41 MJ/kg compared with 16.41 MJ/kg. After torrefaction at 200°C, 250°C, and 300°C, the CV of OPF increases to 17.77 MJ/kg, 20.45 MJ/kg, and 22.46 MJ/kg respectively. On the other hand, the CV of OPT also increases steadily to 19.77 MJ/kg, 21.78 MJ/kg, and 25.48 MJ/kg for temperatures at 200°C, 250°C, and 300°C respectively.

Besides, the experimental CVs obtained were used to compare with the predicted CVs as presented graphically in

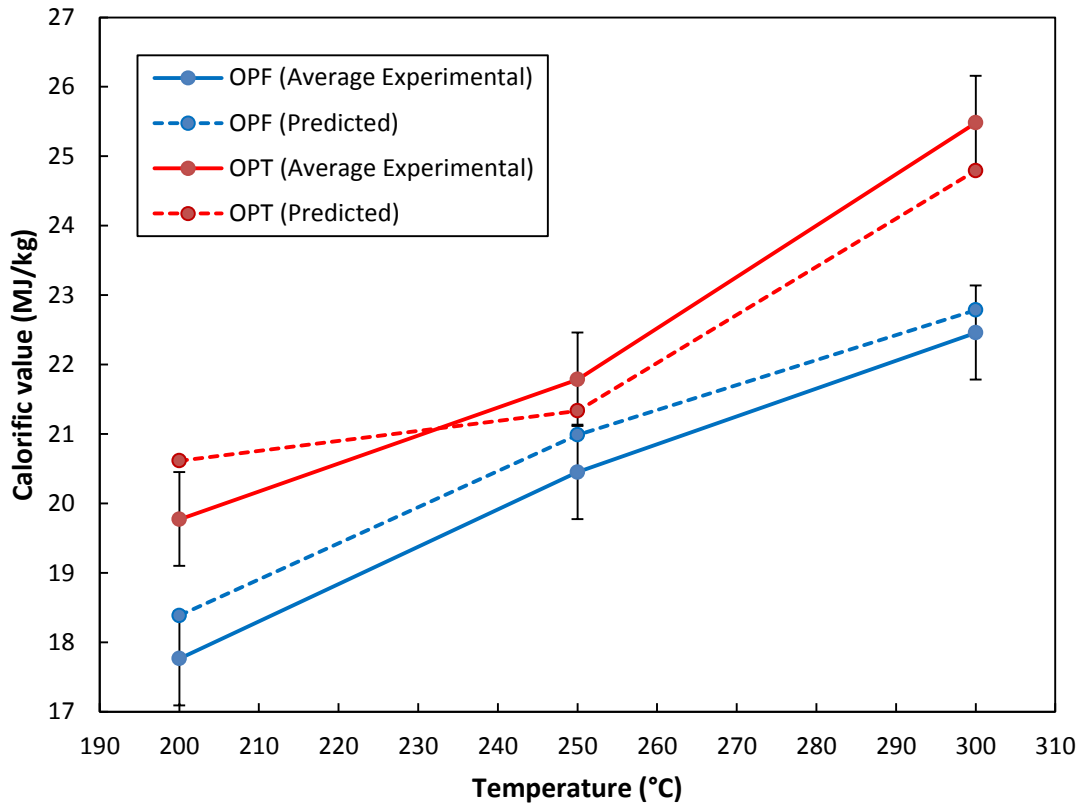


Figure 4-3. As can be seen in Table 4-4, the errors between the predicted and experimental CVs are less than $\pm 5.0\%$. This implies that the self-developed CV predicting tool (CV Predictor v1.0) is applicable for torrefied OPF and OPT in this research work. This tool also validates the experimental CVs which are close to the literature CVs built in the tool itself. Furthermore, the estimation of CV from the colour of torrefied lignocellulosic biomass using RGB colour model is also proven and validated here.

4.5 Effect of Temperature on the Mass and Energy Yields

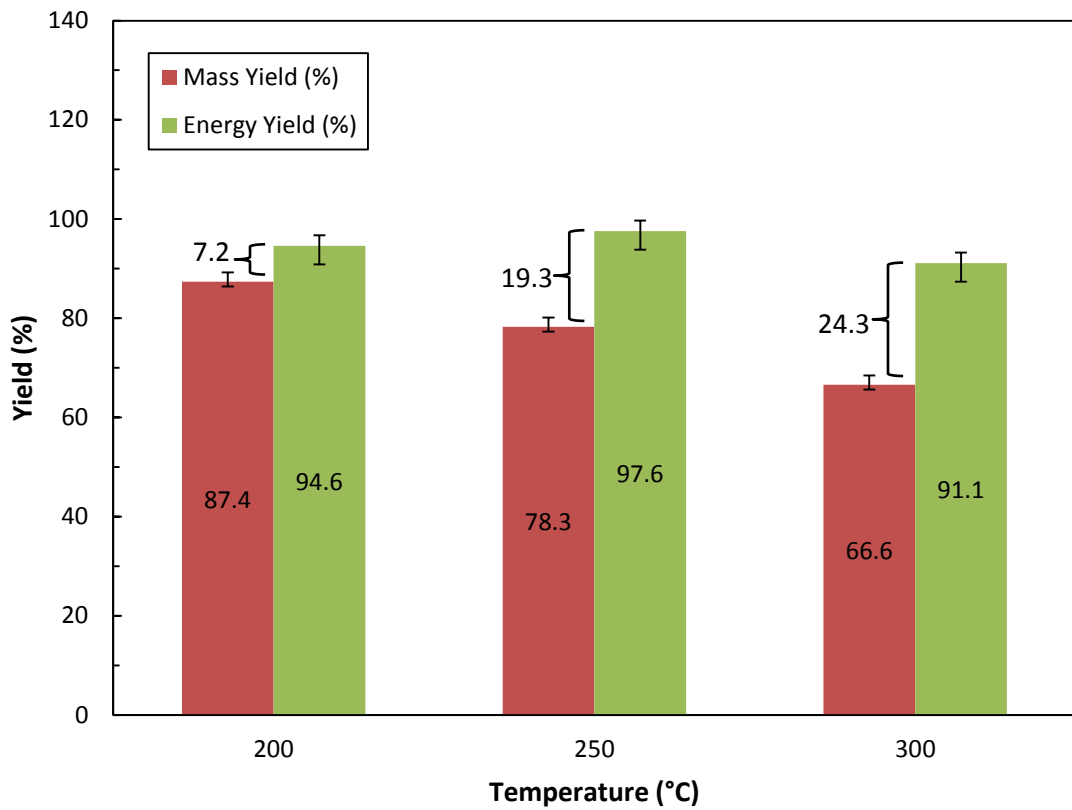


Figure 4-4: Effect of temperature on OPF mass and energy yields (average)

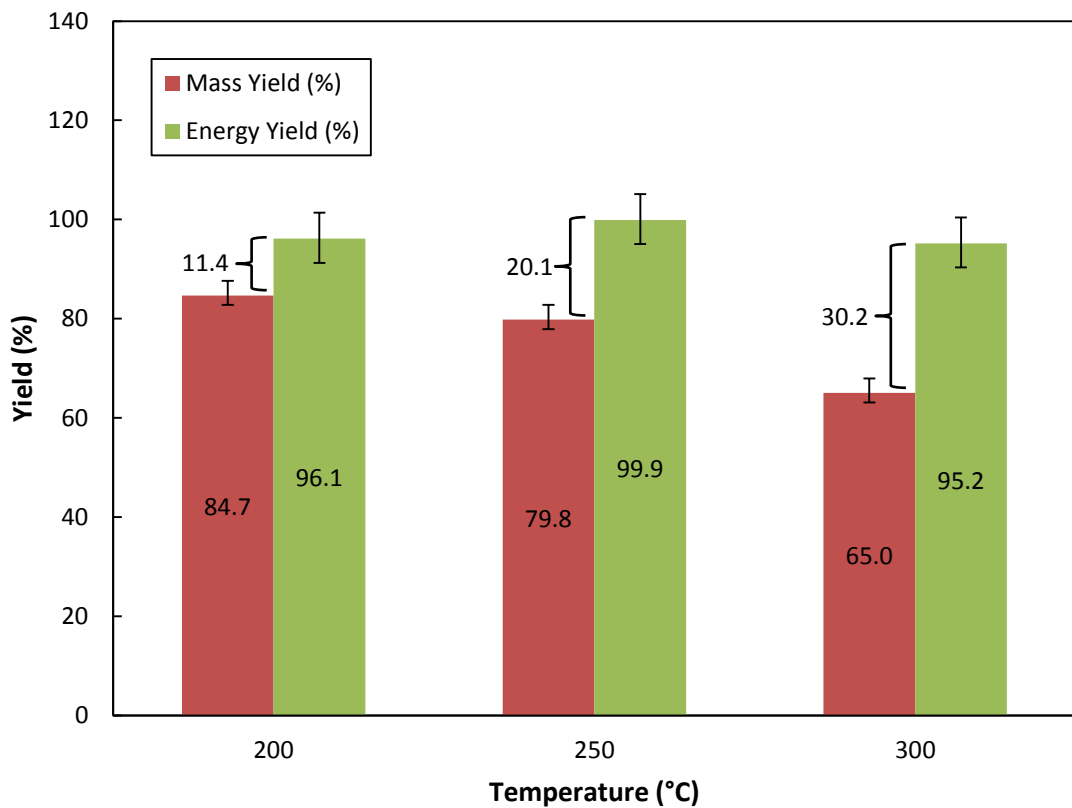


Figure 4-5: Effect of temperature on OPT mass and energy yields (average)

Figure 4-4 and Figure 4-5 show the effects of torrefaction temperature on mass and energy yields of OPF and OPT respectively (please refer Appendix A.1 for detailed tabulated results). The mass yields of both OPF and OPT decrease significantly with elevated torrefaction temperature. It was found that the mass yields for both OPF and OPT decrease at about 20% from 200°C to 300°C, mainly due to liberation of volatile hydrocarbon from rapid thermal decomposition of hemicellulose, cellulose, and some part of lignin. In terms of energy yield, both OPF and OPT were found to maintain their respective energy yield greater than 90%, in spite of different severity of torrefaction treatment (i.e. temperature). The energy yield of the torrefied OPF is remarkably peak at 250°C (97.6%), which is greater compared to the energy yields at 200°C (94.6%) and 300°C (91.1%). The similar case goes to the energy yield of torrefied OPT with remarkably peak at 250°C (99.9%), which is the largest among the other torrefaction temperatures at 200°C (96.1%) and 300°C (95.2%). The gap between mass and energy yield (see Figure 4-4 and Figure 4-5) implies that the mass loss is balanced by the increasing calorific value with elevated torrefaction temperature. Therefore, from this study, the temperature of 250°C gives the best torrefaction result for both OPF and OPT to acquire high energy yield without significant mass loss.

4.6 Fourier Transform Infrared (FTIR) Analysis

Fourier transform infrared spectroscopy was used to investigate changes in functional groups of solid torrefied products. Figure 4-6 and Figure 4-7 show the FTIR spectra of raw and torrefied OPF and OPT recorded in the transmittance mode as a function of wave number in the range of 4000 to 700 cm^{-1} . Peaks are assigned based on literature data (Kobayashi *et al.*, 2009; Yang *et al.*, 2006; Yuliansyah & Hirajima, 2012) (see Appendix A.2). Functional groups of interest are those in the regions where most of the transformation can be observed such as the O-H, C=O, C=C, C-H, and C-O-C groups. Rousset *et al.* (2011) suggested that the most severely treated biomass has its functional group vibrations shifted towards lower intensity.

The intensity of the peak $\sim 3500 \text{ cm}^{-1}$ attributed to O-H groups decreases at elevated temperature, indicating that water molecules within the solids are gradually expelled. In other words, dehydration of the lignocellulosic material occurs. The loss of O-H group

also explains the improved hydrophobicity of torrefied OPF and OPT, and similar decreases in intensity of the O-H vibration have been reported previously for torrefied OPF and OPT (Lai & Idris, 2013). The peak at $\sim 2900\text{ cm}^{-1}$ attributed to aliphatic CH_n groups also weakens at elevated temperature, indicating that several long aliphatic chains are broken down. More distinctive peaks are observed in the region below 2000 cm^{-1} . The peak at $\sim 1700\text{--}1750\text{ cm}^{-1}$ represents carbonyl (C=O) stretching vibrations. In raw OPF and OPT, the vibrations are largely due to the carboxylic acids in hemicelluloses, which can include xyloglucan, arabinoglucuronoxylan, and galactoglucomannan (Van der Stelt *et al.*, 2011). The peak at $\sim 1050\text{ cm}^{-1}$ attributed to glycosidic bonds, indicating the presence of cellulose, steadily weakens and gradually disappears from 250°C to 300°C for both OPF and OPT, indicating that cellulose is partially degraded at this range of temperature. The decrease in intensity for both aromatic skeletal vibrations at $\sim 1520\text{ cm}^{-1}$ and C-O-C aryl-alkyl ether linkages at $\sim 1250\text{ cm}^{-1}$ suggest lignin decomposition (Ibrahim *et al.*, 2013).

By analysing the FTIR spectra of the torrefied samples, it can be concluded that there is no significant structural changes for both OPF and OPT at 200°C and 250°C torrefaction conditions. These low temperature effects however contributed to degradation and depolymerisation of hemicellulose in both OPF and OPT. At 300°C torrefaction condition, hemicellulose is mostly removed and slight degradation of cellulose and lignin is notable at this temperature. The vibration intensity of functional groups for raw and torrefied OPF and OPT is summarized in Table 4-5.

Table 4-5: Vibration intensity of functional groups for raw and torrefied products

Wavenumber (cm^{-1})	Bond	OPF				OPT			
		Raw	200°C	250°C	300°C	Raw	200°C	250°C	300°C
3700-3000	O-H	Very weak	Weak	Medium	Strong	Very weak	Weak	Medium	Strong
3000-2800	C-H	Very weak	Weak	Medium	Strong	Very weak	Weak	Medium	Strong
1800-1650	C=O	Very weak	Weak	Medium	Strong	Very weak	Weak	Medium	Strong
1650-1500	C=C	Very weak	Weak	Medium	Strong	Very weak	Weak	Medium	Strong
1450-1200	C-O-C	Very weak	Weak	Medium	Strong	Very weak	Weak	Medium	Strong
1200-950	C-H	Very weak	Weak	Medium	Strong	Very weak	Weak	Medium	Strong

Very weak Very strong

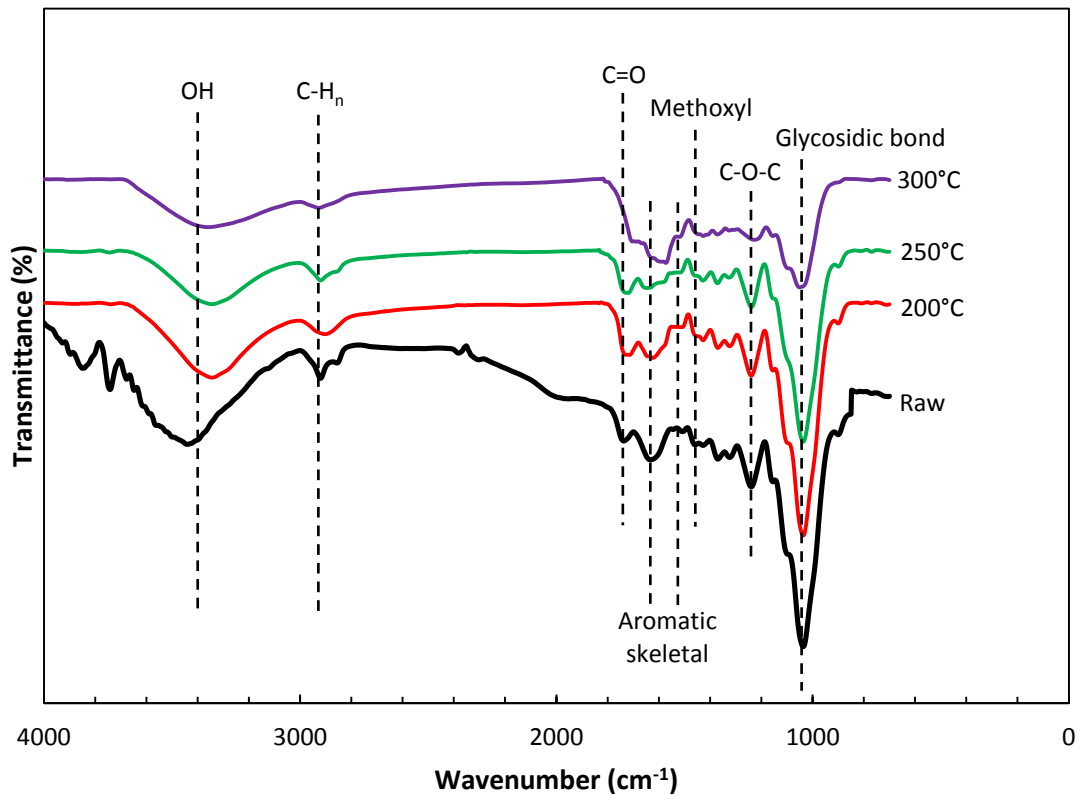


Figure 4-6: FTIR spectra for raw and torrefied OPF at different operating temperature

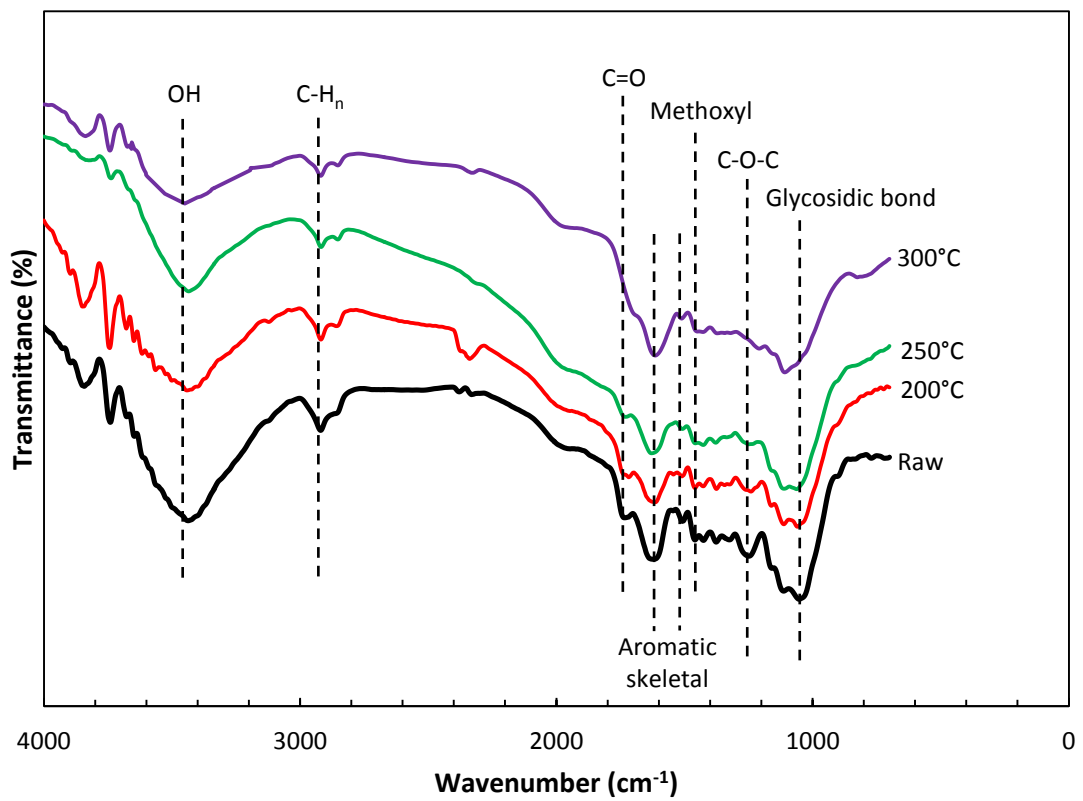


Figure 4-7: FTIR spectra for raw and torrefied OPT at different operating temperature

4.7 Thermogravimetric Analysis (TGA)

Lignocellulosic structure of biomass can be qualitatively identified from thermogravimetry analysis. According to Chen & Kuo (2010) and Zabaniotou *et al.* (2008), weight losses observed in TG and DTG curves are found to be relevant to the composition of cellulose, hemicelluloses, and lignin fractions in lignocellulosic biomass. Residual weight % (TG%) and its first derivative (DTG) of OPF and OPT samples against temperature ranges between 25°C to 800°C at a heating rate of 10°C/min are plotted in Figure 4-8 to Figure 4-11.

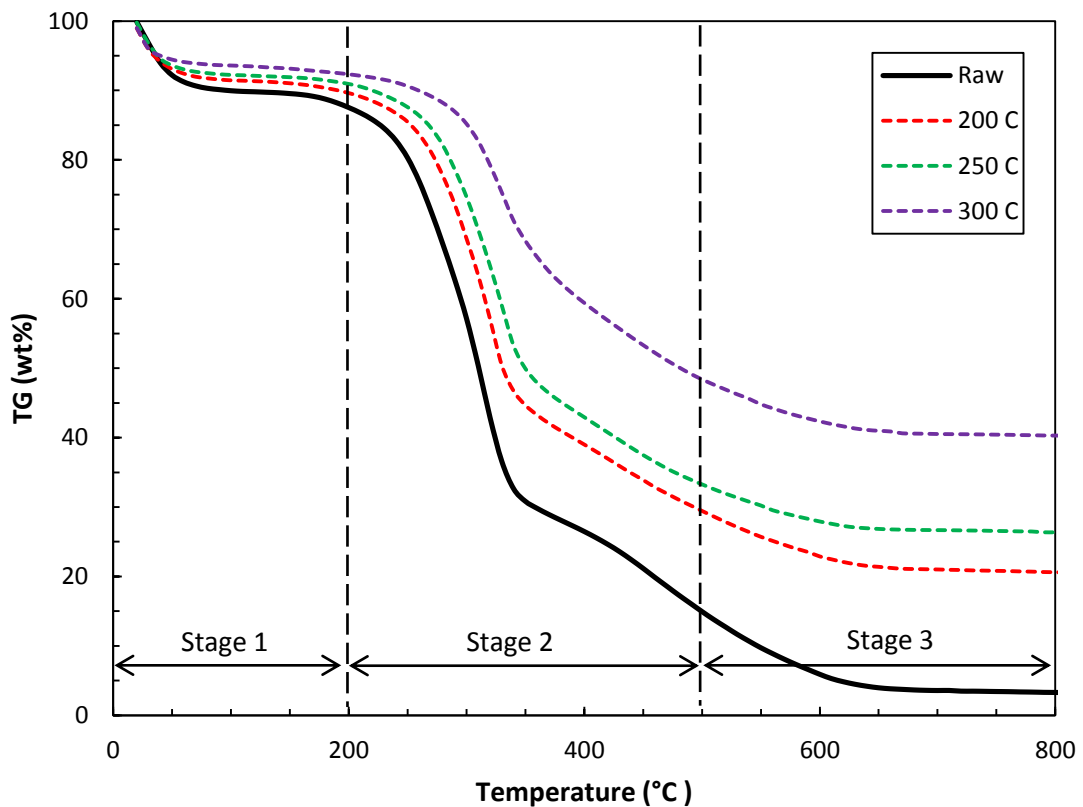


Figure 4-8: TGA curves of raw and torrefied OPF at different operating temperature

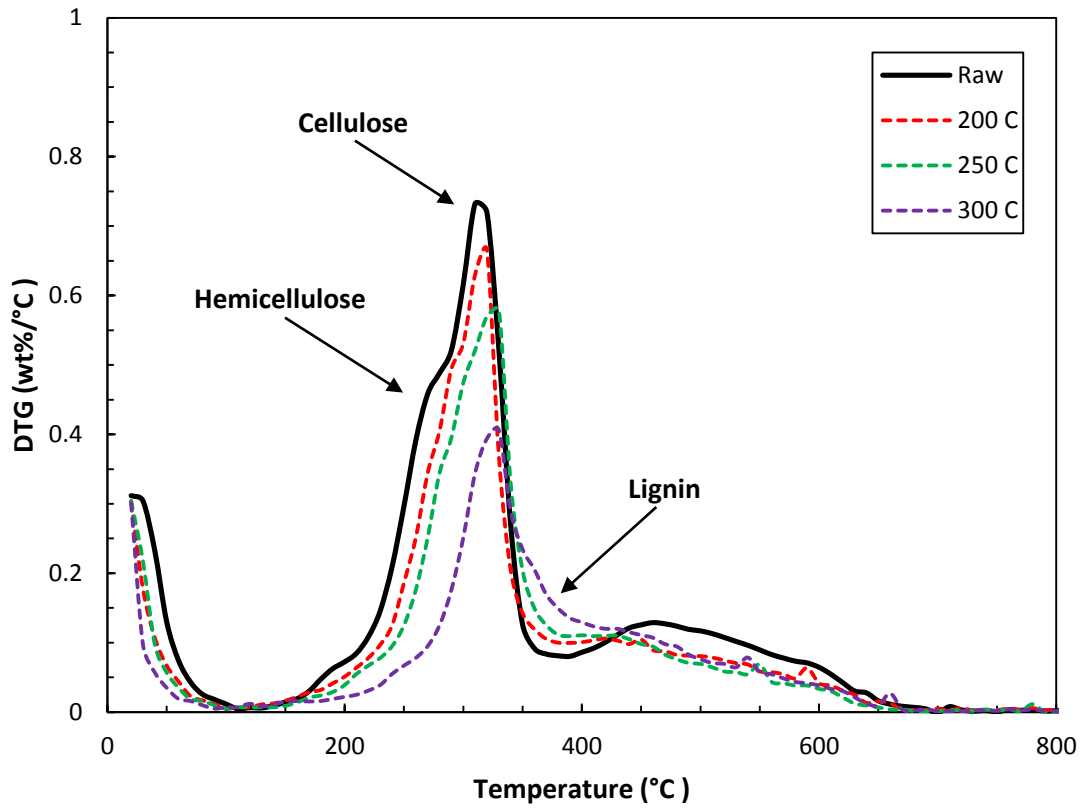


Figure 4-9: DTG curves of raw and torrefied OPF at different operating temperature

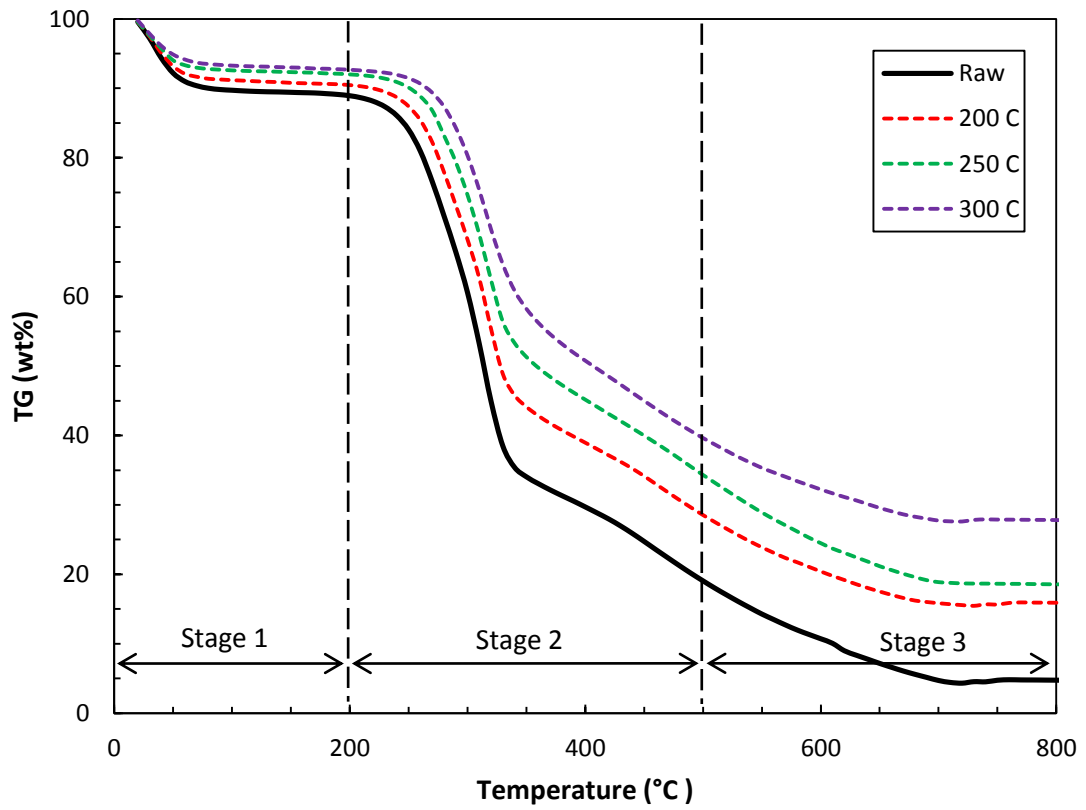


Figure 4-10: TGA curves of raw and torrefied OPT at different operating temperature

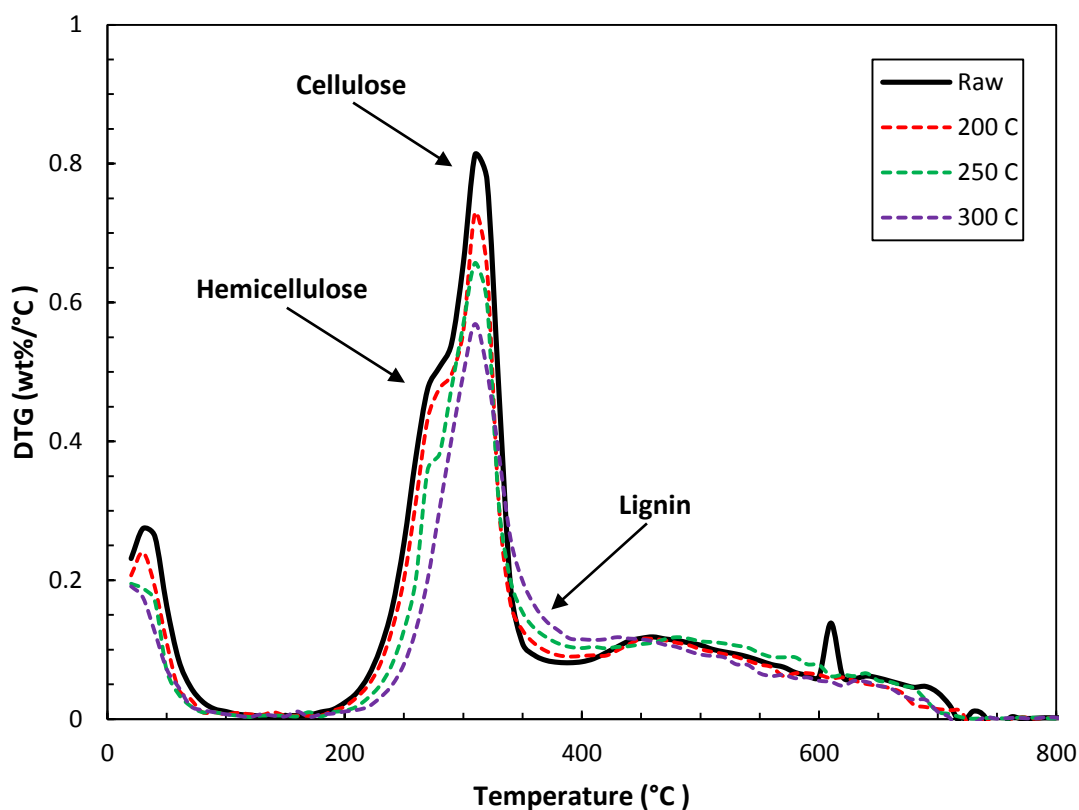


Figure 4-11: DTG curves of raw and torrefied OPT at different operating temperature

In general, three different regions can be distinguished from a particular TG curve. Weight change of a sample was recorded as a function of time or temperature and portrayed by a TG curve. This curve conveys information on thermal behaviour of the torrefied samples. On the other hand, DTG emphasizes the zone of reaction where various reaction steps are taking place over the entire temperature range. In Figure 4-8 and Figure 4-10, different stages of decomposition curves were clearly shown by the dotted vertical lines.

The first stages ($< 200^{\circ}\text{C}$) corresponds to the drying period where highly volatile matter, mainly water were liberated throughout the process. At this early stage, the weight losses for all the tested samples were less than 11% and the weight losses decrease with elevated torrefaction temperature, which result in improved hydrophobicity of torrefied OPF and OPT. Devolatilization is the major step in all thermochemical conversion process involving lignocellulosic biomass. This step is represented by the second stage of decomposition, occurring at temperature ranges between 200 to 500°C , where remarkable slope of the TG curves are observed, corresponding to significant drop in weight of samples due to liberation of volatile hydrocarbon from rapid thermal

decomposition of hemicellulose, cellulose, and some part of lignin. At this stage, weights of the tested samples were reduced to below 40%. This implies that the torrefaction treatment (between 200 to 300°C) has a marked impact upon the lignocellulosic structure, stemming from the thermal degradations of hemicellulose and cellulose.

In examining the DTG curves of the OPF and OPT (Figure 4-9 and Figure 4-11), the thermal degradations of hemicellulose and cellulose can be identified. The peaks of hemicellulose gradually disappear with increasing severity of torrefaction treatment for both OPF and OPT. The severely torrefied OPF and OPT (i.e. at 300°C) contribute the least weight losses, revealing that their resistance against thermal degradation is higher compared to samples torrefied at 200°C and 250°C. For stage 3, weight loss is not as momentous as in stage 2, mainly due to the steady decomposition of the remaining heavy components mainly from lignin.

5 CONCLUSION AND RECOMMENDATION

5.1 Conclusion

This research was experimentally conducted to study the torrefaction effect on physicochemical properties of oil palm fronds (OPF) and oil palm trunks (OPT) at different temperature levels. An extensive study on the effect of biomass colour on calorific value was conducted to develop a CV predicting tool, namely CV Predictor v1.0 using Microsoft Excel spreadsheet. Favourable result has been achieved with less than $\pm 5\%$ error difference between predicted and experimental CV, which validates the accuracy of the CV predicting tool. From the result, the CV of OPF and OPT increases significantly with increasing severity of torrefaction temperature.

Apart from that, mass yields of both materials were found to decrease with increasing torrefaction temperature, indicating that degradation of lignocellulosic components such as hemicellulose, cellulose, and lignin occurs. At a torrefaction temperature of 250°C, the energy yield of the solid product is higher for both OPF and OPT, with 97.6% and 99.9% of the energy retained in the solid materials, respectively. Moreover, the lignocellulosic structures of OPF and OPT were qualitatively identified via Fourier Transform Infrared (FTIR) Spectroscopy, Thermogravimetric analysis (TGA), and Derivative Thermogravimetric (DTG) analysis.

From the analysis, torrefaction process was proven to improve the hydrophobicity of OPF and OPT, which favours the storage and transport applications. Therefore, the oil palm plantation residues, OPF and OPT represents a good source for torrefaction purpose. Also, this process is an attractive method to produce a renewable fuel with favourable properties for gasification and/or co-/combustion applications.

5.2 Recommendation

The following recommendations should be considered throughout this research works. First of all, proper pre-treatment of freshly obtained OPF and OPT should be done accordingly. Once collected, they should be immediately processed into fibre form and properly dried for preservation to prevent biodegradation such as mould and rotting. Improper pre-treatment and preservation methods might influence the experimental result such as FTIR and TGA due to early degradation of lignocellulosic composition.

Besides, in order to increase the accuracy of the CV predicting tool, more data from the previous researches should be found and added. The current CV Predictor v1.0 only applies four data sources to function, which implies that the tool can be further improved to increase its robustness. Apart from that, the handling procedures for bomb calorimeter need to be done accordingly in order to obtain a high precision result for CV. The fuse wire used should be avoided from touching the surface of combustion capsule in the bomb calorimeter which may result in a short circuit that causes the fuse wire to burn before explosion. The length of fuse wire obtained will directly affect the CV of the tested sample.

Furthermore, during the torrefaction process, flushing of nitrogen is compulsory to ensure that the process is carried out in the absence of oxygen. Also, the tubular reactor should be cleaned after each experiment to prevent stain which can cause corrosion in the interior surface of the reactor. The time taken for the cooling process after torrefaction can be shortened by direct blowing with portable fan which effectively reduces the progress delay.

REFERENCES

- Abdullah, N., & Sulaiman, F. (2013). The Oil Palm Wastes in Malaysia, Biomass Now - Sustainable Growth and Use.
- Abdullah, R. (2003). Short-term and long-term projection of Malaysian palm oil production. *Oil Palm Industry Economic Journal*, 32-36.
- Abnisa, F., Arami-Niya, A., Wan Daud, W., Sahu, J., & Noor, I. (2013). Utilization of oil palm tree residues to produce bio-oil and bio-char via pyrolysis. *Energy Conversion And Management*, 1073-1082.
- Acharya, B. (2013). *Torrefaction and Pelletization of Different Forms of Biomass of Ontario*. M,Sc Thesis, School of Engineering, University of Guelph, Ontario, Canada.
- AIM (2011). *National Biomass Strategy 2020: New wealth creation for Malaysia's palm oil industry*. Kuala Lumpur: Agensi Inovasi Malaysia.
- Albizati, K., & Tracewell, C. (2012). Lignin Oxidation and Products Thereof. U.S. Patent 20120107886A1
- Aljuboori, A. (n.d.). Oil Palm Biomass Residue in Malaysia: Availability and Sustainability. *Biomass & Renewables*, 13-18.
- Atnaw, S., Sulaiman, S., & Yusup, S. (2011). Downdraft Gasification of Oil-palm Fronds. *Trends In Applied Sciences Research*, 1006-1018.
- Awan, A., & Khan, Z. (2014). Recent progress in renewable energy--Remedy of energy crisis in Pakistan. *Renewable And Sustainable Energy Reviews*, 236-253.
- Balat, M. (2011). Production of bioethanol from lignocellulosic materials via the biochemical pathway: a review. *Energy Conversion And Management*, 858-875.
- Balat, M., Balat, M., Kirtay, E., & Balat, H. (2009). Main routes for the thermo-conversion of biomass into fuels and chemicals. Part 1: Pyrolysis systems. *Energy Conversion And Management*, 3147-3157.
- Baskar, C., Baskar, S., & Dhillon, R. (2012). *Biomass conversion*. Berlin: Springer.
- Basu, P. (2010). *Biomass gasification and pyrolysis* (1st ed.). Burlington, MA: Academic Press.
- Basyaruddin, M., Ishak, Z., Abdullah, D., Aziz, A., Basri, M., & Salleh, A. (2012). Swelling and dissolution of oil palm biomass in ionic liquids. *Journal of Oil Palm Research*, 1267-1276.
- Bates, R., & Ghoniem, A. (2012). Biomass torrefaction: Modeling of volatile and solid product evolution kinetics. *Bioresource Technology*, 460-469.

- Bergman, P., Prins, M., Boersma, A., Ptasinski, K., Kiel, J., & Janssen, F. (2005). *Torrefaction for entrained-flow gasification of biomass*. Netherlands: Energy Research Centre of the Netherlands (ECN).
- Braber, K. (1995). Anaerobic digestion of municipal solid waste: a modern waste disposal option on the verge of breakthrough. *Biomass And Bioenergy*, 365-376.
- Brebu, M., & Vasile, C. (2010). Thermal degradation of lignin—A review. *Cellulose Chemistry & Technology*, 353-363.
- Chavalparit, O., Ongwandee, M., & Trangkaprasith, K. (2013). Production of Pelletized Fuel from Biodiesel-Production Wastes: Oil Palm Fronds and Crude Glycerin. *EJ*, 61-70.
- Chen, W., & Kuo, P. (2010). A study on torrefaction of various biomass materials and its impact on lignocellulosic structure simulated by a thermogravimetry. *Energy*, 2580-2586.
- Chen, W., & Kuo, P. (2011). Torrefaction and co-torrefaction characterization of hemicellulose, cellulose and lignin as well as torrefaction of some basic constituents in biomass. *Energy*, 803-811.
- Chen, W., Hsu, H., Lu, K., Lee, W., & Lin, T. (2011). Thermal pretreatment of wood (Lauan) block by torrefaction and its influence on the properties of the biomass. *Energy*, 3012-3021.
- Clausen, L., Elmegaard, B., & Houbak, N. (2010). Technoeconomic analysis of a low CO₂ emission dimethyl ether (DME) plant based on gasification of torrefied biomass. *Energy*, 4831-4842.
- Demirbas, A. (2001). Biomass resource facilities and biomass conversion processing for fuels and chemicals. *Energy Conversion And Management*, 1357-1378.
- Demirbas, A. (2008). Biofuels sources, biofuel policy, biofuel economy and global biofuel projections. *Energy Conversion And Management*, 2106-2116.
- Demirbas, A. (2009). *Biohydrogen* (1st ed.). New York: Springer.
- Deng, J., Wang, G., Kuang, J., Zhang, Y., & Luo, Y. (2009). Pretreatment of agriculture residues for co-gasification via torrefaction. *Journal of Analytical and Applied Pyrolysis*, 331-337.
- Dhepe, P., & Sahu, R. (2012). One pot and single step hydrolytic process for the conversion of lignocellulose into value added chemicals. U.S. Patent 20120192860A1
- Diebold, J., & Bridgwater, A. (1997). Overview of fast pyrolysis of biomass for the production of liquid fuels. *Springer*, 5-23.
- Doelle, H. (2003). Biomass and Organic Waste Conversion to Food, Feed, Fuel, Fertilizer, Energy and Commodity Products. *Biotechnology, Ed. Horst W. Doelle*.

- EIA (2013). International Energy Outlook 2013. U.S. Energy Information Administration. Retrieved 6 May 2014, from [http://www.eia.gov/forecasts/ieo/pdf/0484\(2013\).pdf](http://www.eia.gov/forecasts/ieo/pdf/0484(2013).pdf)
- EUBIA (2012). Biomass Characteristics. European Biomass Industry Association (EUBIA). Retrieved 12 May 2014, from <http://www.eubia.org/index.php/about-biomass/biomass-characteristics>
- Ezebor, F., Khairuddean, M., Abdullah, A., & Boey, P. (2014). Oil palm trunk and sugarcane bagasse derived heterogeneous acid catalysts for production of fatty acid methyl esters. *Energy*, 1-11.
- Fauzianto, R. (2014). Implementation of Bioenergy from Palm Oil Waste in Indonesia. *Journal of Sustainable Development Studies*, 100-115.
- Girio, F., Fonseca, C., Carneiro, F., Duarte, L., Marques, S., & Bogel-Lukasik, R. (2010). Hemicelluloses for fuel ethanol: a review. *Bioresource Technology*, 4775-4800.
- Giudicianni, P., Cardone, G., & Ragucci, R. (2013). Cellulose, hemicellulose and lignin slow steam pyrolysis: Thermal decomposition of biomass components mixtures. *Journal Of Analytical And Applied Pyrolysis*, 213-222.
- Goh, C., Lee, K., & Bhatia, S. (2010a). Hot compressed water pretreatment of oil palm fronds to enhance glucose recovery for production of second generation bioethanol. *Bioresource technology*, pp.7362-7367.
- Goh, C., Tan, H., Lee, K., & Mohamed, A. (2010b). Optimizing ethanolic hot compressed water (EHCW) cooking as a pretreatment to glucose recovery for the production of fuel ethanol from oil palm frond (OPF). *Fuel Processing Technology*, 1146-1151.
- Gonzalez-Pena, M., & Hale, M. (2009). Colour in thermally modified wood of beech, Norway spruce and Scots pine. Part 1: Colour evolution and colour changes. *Holzforschung*, 385-393.
- Guangul, F., Sulaiman, S., & Ramli, A. (2012). Gasifier selection, design and gasification of oil palm fronds with preheated and unheated gasifying air. *Bioresource technology*, 224-232.
- Ha, M., Apperley, D., Evans, B., Huxham, I., Jardine, W., & Vietor, R. (1998). Fine structure in cellulose microfibrils: NMR evidence from onion and quince. *The Plant Journal*, 183-190.
- H'ng, P., Wong, L., Chin, K., Tor, E., Tan, S., Tey, B., & Maminski, M. (2011). Oil Palm (*Elaeis guineensis*) Trunk as a Resource of Starch and Other Sugars. *Journal of Applied Sciences*, 3053-3057.
- Ibrahim, R., Darvell, L., Jones, J., & Williams, A. (2013). Physicochemical characterisation of torrefied biomass. *Journal Of Analytical And Applied Pyrolysis*, 21-30.

- Kelly-Yong, T., Lee, K., Mohamed, A., & Bhatia, S. (2007). Potential of hydrogen from oil palm biomass as a source of renewable energy worldwide. *Energy Policy*, 5692-5701.
- Khalil, H., Poh, B., Issam, A., Jawaid, M., & Ridzuan, R. (2010). Recycled polypropylene-oil palm biomass: the effect on mechanical and physical properties. *Journal Of Reinforced Plastics And Composites*, 1117-1130.
- Kobayashi, N., Okada, N., Hirakawa, A., Sato, T., Kobayashi, J., & Hatano, S. et al. (2009). Characteristics of Solid Residues Obtained from Hot-Compressed-Water Treatment of Woody Biomass. *Industrial & Engineering Chemistry Research*, 373-379.
- Kolokolova, O., Levi, T., Pang, S., & Herrington, P. (2013). Torrefaction and Pyrolysis of Biomass Waste in Continuous Reactors. *CEST2013*. Athens, Greece.
- Kucuk, M., & Demirbas, A. (1997). Biomass conversion processes. *Energy Conversion And Management*, 151-165.
- Lai, L., & Idris, A. (2013). Disruption of Oil Palm Trunks and Fronds by Microwave-Alkali Pretreatment. *Bioresources*, 2792-2804.
- Lamaming, J., Hashim, R., Sulaiman, O., Sugimoto, T., Sato, M., & Hiziroglu, S. (2014). Measurement of some properties of binderless particleboards made from young and old oil palm trunks. *Measurement*, 813-819.
- Lim, X., & Andresen, J. (2011). Pyro-catalytic deoxygenated bio-oil from palm oil empty fruit bunch and fronds with boric oxide in a fixed-bed reactor. *Fuel Processing Technology*, 1796-1804.
- Limayem, A., & Ricke, S. (2012). Lignocellulosic biomass for bioethanol production: current perspectives, potential issues and future prospects. *Progress In Energy And Combustion Science*, 449-467.
- Lu, K., Lee, W., Chen, W., Liu, S., & Lin, T. (2012). Torrefaction and low temperature carbonization of oil palm fiber and eucalyptus in nitrogen and air atmospheres. *Bioresource Technology*, 98-105.
- Luo, X. (2011). *Torrefaction of biomass – a comparative and kinetic study of thermal decomposition for Norway spruce stump, poplar and fuel tree chips*. SLU, Swedish University of Agricultural Sciences.
- Mathiesen, B., Lund, H., & Connolly, D. (2012). Limiting biomass consumption for heating in 100% renewable energy systems. *Energy*, 160-168.
- Mohammed, M., Salmiaton, A., Wan Azlina, W., Mohammad Amran, M., Fakhru-Razi, A., & Taufiq-Yap, Y. (2011). Hydrogen rich gas from oil palm biomass as a potential source of renewable energy in Malaysia. *Renewable And Sustainable Energy Reviews*, 1258-1270.

- Mohideen, M., Faiz, M., Salleh, H., Zakaria, H., & Raghavan, V. (2011). Drying of Oil Palm Frond via Swirling Fluidization Technique. *Proceedings of the World Congress on Engineering 2011*, 2375-2380.
- Mokhtar, A., Hassan, K., Aziz, A., & Wahid, M. (2008). Treatment of oil palm lumber. *Malaysian Palm Oil Board (MPOB), Information Series, MPOB TT*, 379.
- MPOB (2011). *Biodiesel and Renewable Energy from Oil Palm*. Retrieved 11 October 2014, from <http://www.mpoc.org.my/upload/Paper3-Dr-Choo.pdf>
- MPOC (2009). Malaysian Palm Oil Industry. Malaysian Palm Oil Council. Retrieved 11 May 2014, from http://www.mpoc.org.my/Malaysian_Palm_Oil_Industry.aspx
- Nhuchhen, D., Basu, P., & Acharya, B. (2014). A Comprehensive Review on Biomass Torrefaction. *International Journal of Renewable Energy & Biofuels*, Article ID 506376, DOI: 10.5171/2014.506376
- Nipattummakul, N., Ahmed, I., Kerdsuwan, S., & Gupta, A. (2010). Hydrogen and syngas production from sewage sludge via steam gasification. *International Journal Of Hydrogen Energy*, 11738-11745.
- Nipattummakul, N., Ahmed, I., Kerdsuwan, S., & Gupta, A. (2012). Steam gasification of oil palm trunk waste for clean syngas production. *Applied Energy*, 778-782.
- Ossai, C., Boswell, B., & Davies, I. (2013). Sustainable asset integrity management: Strategic imperatives for economic renewable energy generation. *Renewable Energy*, 143-152.
- Palmqvist, E., & Hahn-Hagerdal, B. (2000). Fermentation of lignocellulosic hydrolysates. II: inhibitors and mechanisms of inhibition. *Bioresource Technology*, 25-33.
- Peng, J., Bi, H., Sokhansanj, S., & Lim, J. (2012). A study of particle size effect on biomass torrefaction and densification. *Energy & Fuels*, 3826-3839.
- Prins, M., Ptasinski, K., & Janssen, F. (2006). Torrefaction of wood: Part 2. Analysis of products. *Journal Of Analytical And Applied Pyrolysis*, 35-40.
- Rousset, P., Davrieux, F., Macedo, L., & Perré, P. (2011). Characterisation of the torrefaction of beech wood using NIRS: Combined effects of temperature and duration. *Biomass And Bioenergy*, 1219-1226.
- Rowell, R. (2005). *Handbook of wood chemistry and wood composites* (1st ed.). Boca Raton, Fla.: CRC Press.
- Sabil, K., Aziz, M., Lal, B., & Uemura, Y. (2013). Synthetic indicator on the severity of torrefaction of oil palm biomass residues through mass loss measurement. *Applied Energy*, 821-826.
- Salim, N., Hashim, R., Sulaiman, O., Nordin, N., Ibrahim, M., & Md Akil, H. (2013). Effect of Steaming on Some Properties of Compressed Oil Palm Trunk Lumber. *Bioresources*, 2310-2324.

- Sanchez, C. (2009). Lignocellulosic residues: biodegradation and bioconversion by fungi. *Biotechnology Advances*, 185-194.
- Sime Darby (2014). Palm Oil Facts & Figures. Retrieved 18 May 2014, from http://www.simedarby.com/upload/Palm_Oil_Facts_and_Figures.pdf
- Singh, T., Singh, A., Hussain, I., & Hall, P. (2013). Chemical characterisation and durability assessment of torrefied radiata pine (*Pinus radiata*) wood chips. *International Biodeterioration & Biodegradation*, 347-353.
- Sopian, K., Othman, M., & Yatim, B. (2000). *Renewable Energy – Resources and Applications in Malaysia*. Kajang: Pusat Tenaga Malaysia.
- Sorum, L., Gronli, M., & Hustad, J. (2001). Pyrolysis characteristics and kinetics of municipal solid wastes. *Fuel*, 1217-1227.
- Srirangan, K., Akawi, L., Moo-Young, M., & Chou, C. (2012). Towards sustainable production of clean energy carriers from biomass resources. *Applied Energy*, 172-186.
- Stelte, W. (2012). *Torrefaction of unutilized biomass resources and characterization of torrefaction gasses*. Resultat Kontrakt (RK) Report. Danish Technological Institute. Retrieved 12 October 2014, from http://www.teknologisk.dk/_root/media/52684_RK%20report%20torrefaction%20and%20torrefaction%20gas.pdf
- Stelte, W., Clemons, C., Holm, J., Sanadi, A., Ahrenfeldt, J., Shang, L., & Henriksen, U. (2011). Pelletizing properties of torrefied spruce. *Biomass And Bioenergy*, 4690-4698.
- Sulaiman, O., Salim, N., Hashim, R., Yusof, L., Razak, W., & Yunus, N. (2009). Evaluation on the suitability of some adhesives for laminated veneer lumber from oil palm trunks. *Materials & Design*, 3572-3580.
- Sun, Y., & Cheng, J. (2002). Hydrolysis of lignocellulosic materials for ethanol production: a review. *Bioresource Technology*, 1-11.
- Tomme, P., Warren, R., & Gilkes, N. (1995). Cellulose hydrolysis by bacteria and fungi. *Advances In Microbial Physiology*, 1-81.
- Toor, S., Rosendahl, L., & Rudolf, A. (2011). Hydrothermal liquefaction of biomass: a review of subcritical water technologies. *Energy*, 2328-2342.
- Tumuluru, J., Sokhansanj, S., Hess, J., Wright, C., & Boardman, R. (2011). REVIEW: A review on biomass torrefaction process and product properties for energy applications. *Industrial Biotechnology*, 384-401.
- UNEP (2012). *Converting Waste Oil Palm Trees into A Resource*. United Nations Environment Programme. Retrieved 12 October 2014, from http://www.unep.org/ietc/Portals/136/News/Waste%20Palm%20Tree%20study%20report%20publication/Converting%20Waste%20Oil%20Palm%20into%20a%20Resource_FINAL%20REPORT.pdf

- Van der Stelt, M., Gerhauser, H., Kiel, J., & Ptasinski, K. (2011). Biomass upgrading by torrefaction for the production of biofuels: a review. *Biomass And Bioenergy*, 3748-3762.
- Veign. (2009). *Pixeur: Color picker to determine a pixel's color (v3.2.0.0)*. Retrieved 19 December 2014, from <http://www.veign.com/application.php?appid=107>
- Wang, C., Peng, J., Li, H., Bi, X., Legros, R., Lim, C., & Sokhansanj, S. (2013). Oxidative torrefaction of biomass residues and densification of torrefied sawdust to pellets. *Bioresource Technology*, 318-325.
- Wang, M., Huang, Y., Chiueh, P., Kuan, W., & Lo, S. (2012). Microwave-induced torrefaction of rice husk and sugarcane residues. *Energy*, 177-184.
- Wannapeera, J., Fungtammasan, B., & Worasuwanarak, N. (2011). Effects of temperature and holding time during torrefaction on the pyrolysis behaviors of woody biomass. *Journal Of Analytical And Applied Pyrolysis*, 99-105.
- Wanrosli, W., Zainuddin, Z., Law, K., & Asro, R. (2007). Pulp from oil palm fronds by chemical processes. *Industrial crops and products*, 89-94.
- Wyman, C. (2013). *Aqueous Pretreatment of Plant Biomass for Biological and Chemical Conversion to Fuels and Chemicals* (1st ed.). Chichester: Wiley.
- Xue, G., Kwapinska, M., Kwapinski, W., Czajka, K., Kennedy, J., & Leahy, J. (2014). Impact of torrefaction on properties of *Miscanthus × giganteus* relevant to gasification. *Fuel*, 189-197.
- Yang, H., Yan, R., Chen, H., Lee, D., & Zheng, C. (2007). Characteristics of hemicellulose, cellulose and lignin pyrolysis. *Fuel*, 1781-1788.
- Yang, H., Yan, R., Chen, H., Lee, D., Liang, D., & Zheng, C. (2006). Pyrolysis of palm oil wastes for enhanced production of hydrogen rich gases. *Fuel Processing Technology*, 935-942.
- Yuliansyah, A., & Hirajima, T. (2012). Efficacy of Hydrothermal Treatment for Production of Solid Fuel from Oil Palm Wastes. *Resource Management for Sustainable Agriculture*.
- Zabaniotou, A., Ioannidou, O., Antonakou, E., & Lappas, A. (2008). Experimental study of pyrolysis for potential energy, hydrogen and carbon material production from lignocellulosic biomass. *International Journal Of Hydrogen Energy*, 2433-2444.
- Zahari, M., Hassan, O., Wong, H., & Liang, J. (2003). Utilization of oil palm frond-based diets for beef and dairy production in Malaysia. *ASIAN AUSTRALASIAN JOURNAL OF ANIMAL SCIENCES*, 625-634.

APPENDICES

Appendix A.1: Summary of experimental results

A.1.1: Results of CV, mass and energy yield

<i>Type of sample</i>	<i>Temperature (°C)</i>	<i>Sample no.</i>	<i>CV (MJ/kg)</i>	<i>CV ratio</i>	<i>Mass yield (%)</i>	<i>Energy yield (%)</i>	
OPF	200	1	17.0904	1.0417	87.22	90.85	
		2	18.1042	1.1035	87.50	96.56	
		3	18.1004	1.1032	87.35	96.36	
	Average			17.7650	1.0828	87.36	94.59
	250	1	20.1241	1.2266	77.32	94.84	
		2	21.1341	1.2881	77.41	99.72	
		3	20.0952	1.2248	80.15	98.17	
	Average			20.4511	1.2465	78.29	97.57
	300	1	23.1290	1.4097	66.14	93.24	
		2	22.1152	1.3479	67.05	90.37	
		3	22.1286	1.3487	66.57	89.79	
	Average			22.4576	1.3688	66.58	91.13
OPT	200	1	20.1068	1.1548	82.77	95.59	
		2	19.1026	1.0972	86.15	94.52	
		3	20.1049	1.1547	85.11	98.28	
	Average			19.7714	1.1356	84.68	96.13
	250	1	22.1209	1.2705	82.76	105.14	
		2	21.1091	1.2124	78.39	95.04	
		3	22.1229	1.2706	78.30	99.49	
	Average			21.7843	1.2512	79.82	99.89
	300	1	25.1489	1.4444	64.62	93.33	
		2	26.1608	1.5025	65.61	98.58	
		3	25.1373	1.4438	64.81	93.57	
	Average			25.4823	1.4636	65.01	95.16

The following tables refer to the data recorded from bomb calorimeter experiments.

A.1.2: OPF (Before torrefaction)

	Sample 1	Sample 2	Sample 3
Mass of sample (gram)	0.50	0.50	0.50
Unburned fuse wire (cm)	2.90	3.10	3.00

Time (minute)	Temperature reading (°C)		
	Sample 1	Sample 2	Sample 3
0	27.50	29.20	29.10
1	27.80	29.50	29.40
2	28.20	29.80	29.75
3	28.25	29.95	29.85
4	28.30	30.00	29.90
5	28.30	30.00	29.95
6	28.30	30.00	29.95
7	–	–	29.95

A.1.3: OPT (Before torrefaction)

	Sample 1	Sample 2	Sample 3
Mass of sample (gram)	0.50	0.50	0.50
Unburned fuse wire (cm)	3.20	3.00	3.40

Time (minute)	Temperature reading (°C)		
	Sample 1	Sample 2	Sample 3
0	30.40	30.45	30.25
1	30.70	30.70	30.60
2	30.95	31.05	30.85
3	31.15	31.25	31.00
4	31.20	31.30	31.05
5	31.25	31.35	31.10
6	31.25	31.35	31.10
7	31.25	31.35	31.10

A.1.4: OPF (After torrefaction at 200°C)

	Sample 1	Sample 2	Sample 3
Mass of sample (gram)	0.50	0.50	0.50
Unburned fuse wire (cm)	2.40	2.10	2.30

Time (minute)	Temperature reading (°C)		
	Sample 1	Sample 2	Sample 3
0	27.50	28.35	28.55
1	27.75	28.55	29.05
2	28.15	28.95	29.35
3	28.25	29.10	29.40
4	28.30	29.20	29.45
5	28.35	29.25	29.45
6	28.35	29.25	29.45
7	28.35	29.25	–

A.1.5: OPT (After torrefaction at 200°C)

	Sample 1	Sample 2	Sample 3
Mass of sample (gram)	0.50	0.50	0.50
Unburned fuse wire (cm)	2.80	2.60	2.90

Time (minute)	Temperature reading (°C)		
	Sample 1	Sample 2	Sample 3
0	28.75	28.20	28.45
1	29.15	28.55	28.75
2	29.45	28.85	29.05
3	29.65	28.00	29.30
4	29.70	29.10	29.40
5	29.75	29.15	29.45
6	29.75	29.15	29.45
7	29.75	29.15	29.45

A.1.6: OPF (After torrefaction at 250°C)

	Sample 1	Sample 2	Sample 3
Mass of sample (gram)	0.50	0.50	0.50
Unburned fuse wire (cm)	1.90	1.80	3.40

Time (minute)	Temperature reading (°C)		
	Sample 1	Sample 2	Sample 3
0	28.25	28.50	28.10
1	28.70	28.70	28.35
2	29.05	29.05	28.80
3	29.20	29.40	28.95
4	29.25	29.50	29.05
5	29.25	29.55	29.10
6	29.25	29.55	29.10
7	–	29.55	29.10

A.1.7: OPT (After torrefaction at 250°C)

	Sample 1	Sample 2	Sample 3
Mass of sample (gram)	0.50	0.50	0.50
Unburned fuse wire (cm)	2.90	3.10	2.80

Time (minute)	Temperature reading (°C)		
	Sample 1	Sample 2	Sample 3
0	29.45	29.70	28.90
1	29.85	30.05	29.35
2	30.25	30.35	29.70
3	30.40	30.55	29.85
4	30.45	30.65	29.95
5	30.50	30.70	30.00
6	30.55	30.75	30.00
7	30.55	30.75	30.00
8	30.55	30.75	–

A.1.8: OPF (After torrefaction at 300°C)

	Sample 1	Sample 2	Sample 3
Mass of sample (gram)	0.50	0.50	0.50
Unburned fuse wire (cm)	2.90	3.20	2.50

Time (minute)	Temperature reading (°C)		
	Sample 1	Sample 2	Sample 3
0	27.45	27.90	27.60
1	27.80	28.20	27.95
2	28.30	28.60	28.35
3	28.45	28.85	28.55
4	28.55	28.95	28.65
5	28.60	29.00	28.70
6	28.60	29.00	28.70
7	28.60	29.00	28.70

A.1.9: OPT (After torrefaction at 300°C)

	Sample 1	Sample 2	Sample 3
Mass of sample (gram)	0.50	0.50	0.50
Unburned fuse wire (cm)	2.70	2.50	3.30

Time (minute)	Temperature reading (°C)		
	Sample 1	Sample 2	Sample 3
0	28.25	29.10	29.30
1	28.75	29.45	29.65
2	29.20	29.95	30.05
3	29.35	30.20	30.35
4	29.40	30.30	30.45
5	29.45	30.35	30.50
6	29.50	30.40	30.55
7	29.50	30.40	30.55
8	29.50	30.40	30.55

Appendix A.2: Characteristic of IR Absorptions / Transmittances

A.2.1: Identification of functional groups at various wavenumber ranges

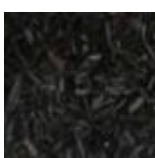
Wavenumber, cm^{-1}	Bond	Functional group
3640–3610 (s, sh)	O–H stretch, free hydroxyl	alcohols, phenols
3500–3200 (s,b)	O–H stretch, H-bonded	alcohols, phenols
3400–3250 (m)	N–H stretch	1°, 2° amines, amides
3300–2500 (m)	O–H stretch	carboxylic acids
3330–3270 (n, s)	–C≡C–H: C–H stretch	alkynes (terminal)
3100–3000 (s)	C–H stretch	aromatics
3100–3000 (m)	=C–H stretch	alkenes
3000–2850 (m)	C–H stretch	alkanes
2830–2695 (m)	H–C=O: C–H stretch	aldehydes
2260–2210 (v)	C≡N stretch	nitriles
2260–2100 (w)	–C≡C– stretch	alkynes
1760–1665 (s)	C=O stretch	carbonyls (general)
1760–1690 (s)	C=O stretch	carboxylic acids
1750–1735 (s)	C=O stretch	esters, saturated aliphatic
1740–1720 (s)	C=O stretch	aldehydes, saturated aliphatic
1730–1715 (s)	C=O stretch	α, β-unsaturated esters
1715 (s)	C=O stretch	ketones, saturated aliphatic
1710–1665 (s)	C=O stretch	α, β-unsaturated aldehydes, ketones
1680–1640 (m)	–C=C– stretch	alkenes
1650–1580 (m)	N–H bend	1° amines
1600–1585 (m)	C–C stretch (in-ring)	aromatics
1550–1475 (s)	N–O asymmetric stretch	nitro compounds
1500–1400 (m)	C–C stretch (in-ring)	aromatics
1470–1450 (m)	C–H bend	alkanes
1370–1350 (m)	C–H rock	alkanes
1360–1290 (m)	N–O symmetric stretch	nitro compounds
1335–1250 (s)	C–N stretch	aromatic amines
1320–1000 (s)	C–O stretch	alcohols, carboxylic acids, esters, ethers
1300–1150 (m)	C–H wag (–CH ₂ X)	alkyl halides
1250–1020 (m)	C–N stretch	aliphatic amines
1000–650 (s)	=C–H bend	alkenes
950–910 (m)	O–H bend	carboxylic acids
910–665 (s, b)	N–H wag	1°, 2° amines
900–675 (s)	C–H “oop”	aromatics
850–550 (m)	C–Cl stretch	alkyl halides
725–720 (m)	C–H rock	alkanes
700–610 (b, s)	–C≡C–H: C–H bend	alkynes
690–515 (m)	C–Br stretch	alkyl halides

m=medium, w=weak, s=strong, n=narrow, b=broad, sh=sharp

Appendix A.3: Colour Characterization Data

A.3.1: Colour and CV of various lignocellulosic biomass

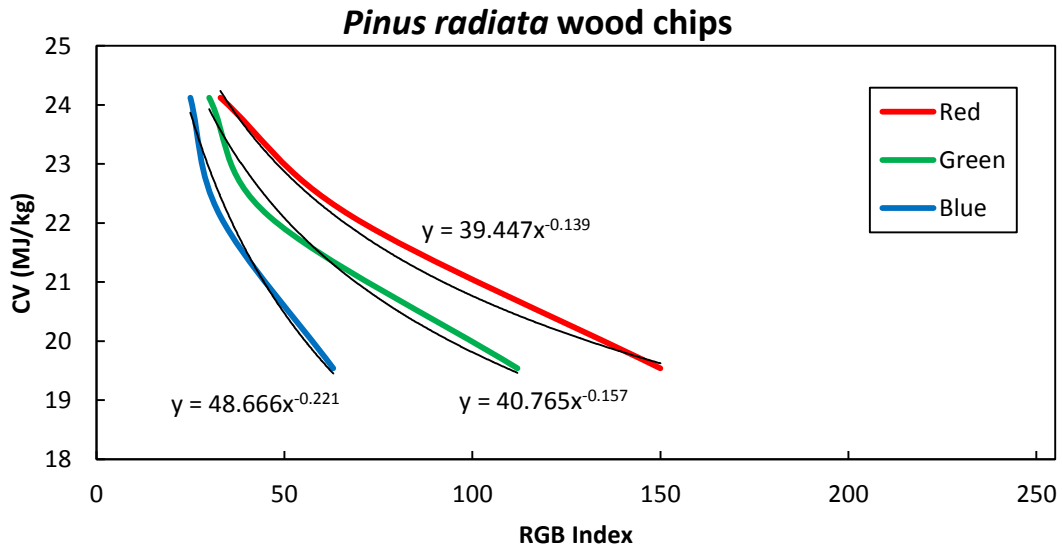
<i>Material Type</i>	<i>Characteristic</i>	<i>RGB</i>	<i>Source</i>
<i>Pinus radiata</i> wood chips	 Raw 17.23 MJ/kg	R: 230 G: 212 B: 180	(Singh <i>et al.</i> , 2013)
	 220°C 19.54 MJ/kg	R: 150 G: 112 B: 63	
	 260°C 22.21 MJ/kg	R: 68 G: 46 B: 33	
	 300 °C 24.12 MJ/kg	R: 33 G: 30 B: 25	
Poplar	 200°C 19.05 MJ/kg	R: 205 G: 178 B: 109	(Luo, 2011)
	 250°C 20.62 MJ/kg	R: 98 G: 78 B: 59	
	 300°C 22.12 MJ/kg	R: 48 G: 50 B: 42	

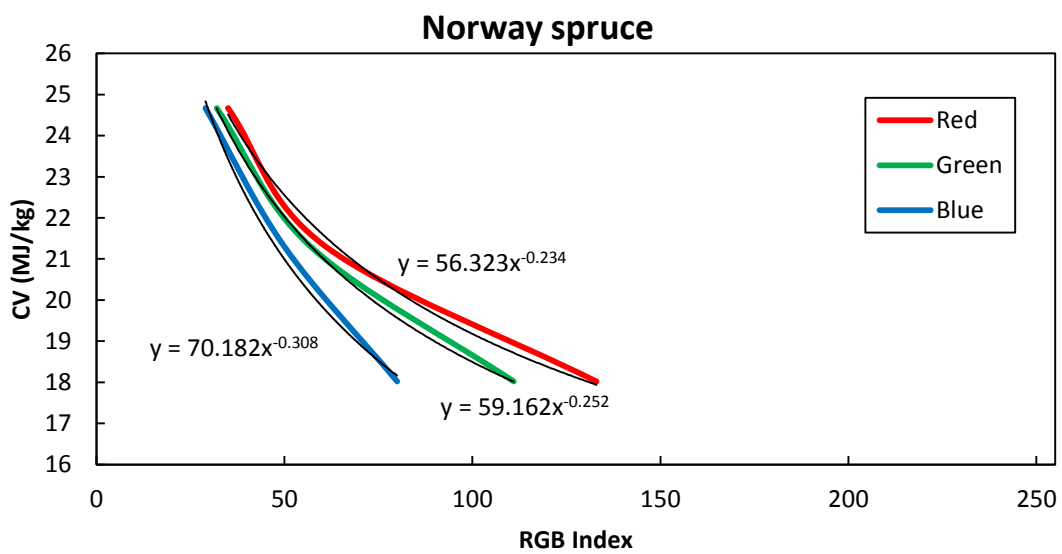
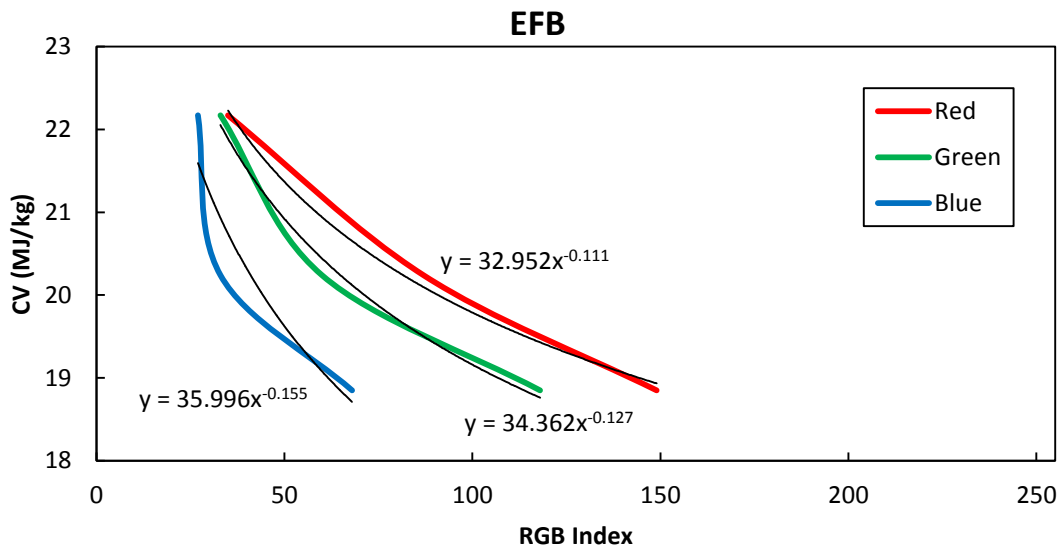
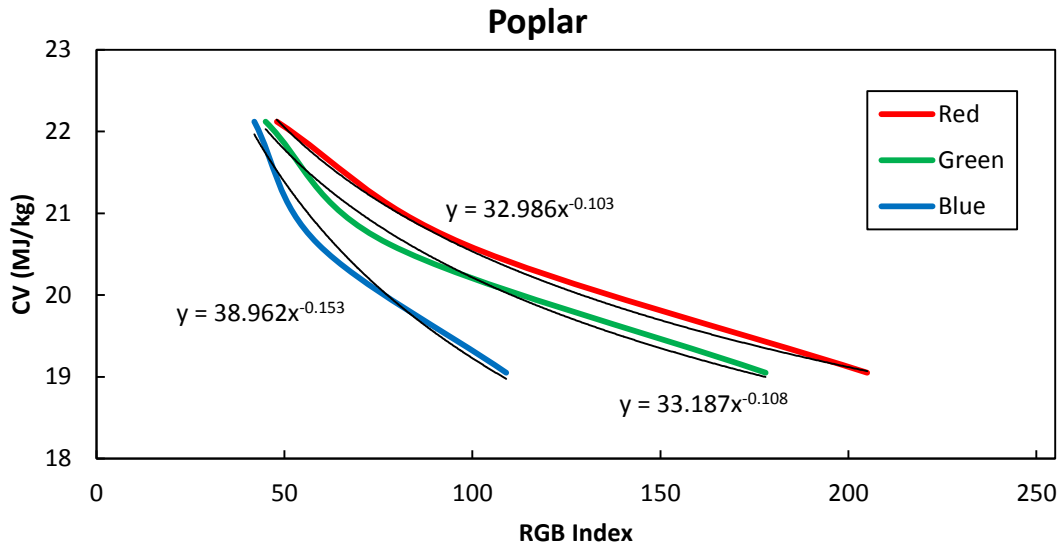
Oil palm empty fruit bunch (EFB)		Raw 17.02 MJ/kg	R: 192 G: 162 B: 94	(Stelte, 2012)
		220°C 18.85 MJ/kg	R: 149 G: 118 B: 68	
		250°C 20.24 MJ/kg	R: 87 G: 60 B: 33	
		300°C 22.17 MJ/kg	R: 35 G: 33 B: 27	
Norway spruce		Raw 16.38 MJ/kg	R: 201 G: 185 B: 156	(Stelte <i>et al.</i> , 2011)
		250°C 18.02 MJ/kg	R: 133 G: 111 B: 80	
		275°C 21.30 MJ/kg	R: 61 G: 57 B: 50	
		300°C 24.67 MJ/kg	R: 35 G: 32 B: 29	

A.3.2: Identification of functional groups at various wavenumber ranges

Material Type	Temperature	RGB Index			CV
	°C	Red	Green	Blue	MJ/kg
<i>Pinus radiata</i> wood chips	25	230	212	180	17.23
	220	150	112	63	19.54
	260	68	46	33	22.11
	300	33	30	25	24.12
Poplar	25	-	-	-	-
	200	205	178	109	19.05
	250	98	78	59	20.62
EFB	25	192	162	94	17.02
	220	149	118	68	18.85
	250	87	60	33	20.24
	300	35	33	27	22.17
Norway spruce	25	201	185	156	16.38
	250	133	111	80	18.02
	275	61	57	50	21.3
	300	35	32	29	24.67

The following graphs refer to the data obtained from A.3.2 to develop equations of CV as a function of RGB index. The equations are used to further develop a CV predicting tool, namely CV Predictor v1.0 for this study.





The power functions of CV obtained from the graphs above are presented by:

$$CV_i = A \times i^B$$

where A and B are constants which can be obtained from the graphs.

By specifying the values of R, G, and B, the calorific value (CV) can be calculated using the equation below.

$$CV = \frac{CV_R + CV_G + CV_B}{3}$$

where

$$CV_R = \frac{1}{4} (39.446 R^{-0.139} + 32.986 R^{-0.103} + 32.952 R^{-0.111} + 56.323 R^{-0.234})$$

$$CV_G = \frac{1}{4} (40.765 G^{-0.157} + 33.187 G^{-0.108} + 34.362 G^{-0.127} + 59.162 G^{-0.252})$$

$$CV_B = \frac{1}{4} (48.666 B^{-0.221} + 38.962 B^{-0.155} + 35.996 B^{-0.155} + 70.182 B^{-0.308})$$

The finished CV predicting tools, CV Predictor v1.0 created using Microsoft Excel spreadsheet is shown in A.3.3 below.

A.3.3: CV Predictor created using Microsoft Excel spreadsheet